Summer 2017

Reduction of tetrachloroethylene and trichloroethylene by magnetite revisted

Johnathan D Culpepper
University of Iowa

REDUCTION OF TETRACHLOROETHYLENE AND TRICHLOROETHYLENE BY MAGNETITE REVISTED

by

Johnathan D. Culpepper

A thesis submitted in partial fulfillment
of the requirements for the Master of Science
degree in Civil and Environmental Engineering in the
Graduate College of
The University of Iowa

August 2017

Thesis Supervisor: Associate Professor Michelle M. Scherer

Graduate College
The University of Iowa
Iowa City, Iowa

CERTIFICATE OF APPROVAL

_____

MASTER'S THESIS

_____

This is to certify that the Master's thesis of

Johnathan D. Culpepper

has been approved by the Examining Committee for
the thesis requirement for the Master of Science degree
in Civil and Environmental Engineering at the August 2017 graduation.

Thesis Committee: _____
Michelle M. Scherer, Thesis Supervisor

_____
Craig Just

_____
Drew E. Latta

To my parents, wife, and children.

ACKNOWLEDGEMENTS

I would like to thank my advisor, Dr. Michelle Scherer for granting me the opportunity to work and develop as a researcher within her laboratory. She has taught me a great deal about Environmental engineering, especially with the intricacies of iron-based and aquatic geochemistry, experimental design, and the importance of effective scientific communication for the professional and public communities. These are all transferable skills, which I will take with me as I pursue a PhD degree in Chemistry.

I would also like to thank Dr. Drew Latta for his insightfulness and guidance, as he assisted me to develop the necessary skills for chlorinated solvent and mineralogical analytical methods. At times, he has challenged me and provided invaluable guidance towards the interruption of data. I would also like to thank Dr. Craig Just, who has taught me Environmental organic chemistry, and has agreed to be a part of my thesis committee.

Thank you to the Department of Civil and Environmental Engineering (CEE) administrative staff Kimberly Lebeck and Jennifer Rumping for all their assistance. To the IIHR-Hydroscience and engineering thank you, for allowing me to be a part of such an amazing world-renowned center for learning.

Finally, thank you to the National Science Foundation, Graduate Research Fellowship program (NSF-GFRP) for being an amazing resource. I will also like to acknowledge the National GEM Consortium for accepting me as an Associate Fellow.

This research has been funded entirely with funds from the Department of Defense Strategic Environmental Research and Development Program – (SERDP), and the NSF-GFRP.

ABSTRACT

For this study, we revisited whether the common iron Fe mineral, magnetite Fe_3O_4 (s), can reduce tetrachloroethylene (PCE) and trichloroethylene (TCE) as discrepancies exist in the literature regarding rates and extent of reduction. We measured PCE and TCE reduction in batch reactors as a function of magnetite stoichiometry (x = Fe^{2+}/Fe^{3+} ratio), solids loading, pH, and Fe(II) concentration. Our results show that magnetite reacts only slowly with TCE ($t_{1/2}$ = 7.6 years) and is not reactive with PCE over 150 days. The addition of aqueous Fe(II) to magnetite suspensions, however, results in slow, but measurable PCE and TCE reduction under some conditions. The solubility of ferrous hydroxide, $Fe(OH)_2$(s), appears to play an important role in whether magnetite reduces PCE and TCE. In addition, we found that $Fe(OH)_2$(s) reduces PCE and TCE at high Fe(II) concentrations as well. At certain conditions degradation of the PCE and TCE is enhanced by an unexplored synergistic response from magnetite and ferrous hydroxide iron phases. Our work suggests that measuring dissolved Fe(II) concentration and pH may be used as indicators to predict whether PCE and TCE will be abiotically degraded by groundwater aquifer solids containing magnetite.

PUBLIC ABSTRACT

Groundwater aquifers with toxic chlorinated solvents is an old problem. But today the most frequently detected volatile organic compounds (VOC) in aquifers are tetrachloroethylene (PCE) and trichloroethylene (TCE), also known as chlorinated ethenes (CE). Conventional remediation like pump and treat has a high carbon footprint, and is unlikely to meet regulated standards. To reduce the environmental impact for treating contaminated groundwater, we explored alternatives with ferrous iron [Fe(II)] bearing minerals, like magnetite to catalyze CE removal. Active research on Fe(II)-bearing minerals, have advanced our understanding for groundwater remedies for natural attenuation and engineered systems. Knowledge gaps exist towards the predictability of mineral-specific processes, and how they contribute to removal of CEs. The first field based evidence for natural non-biological degradation of a CEs with Fe(II)-bearing minerals, was from sediments containing magnetite. Magnetite with Fe^{2+}/Fe^{3+} ratio (x) of 0.5 has greatest potential to reduce PCE and TCE, however, few studies report the solid-state ratio when performing experiments with magnetite. In this study, we measured PCE/TCE removal in batch reactors as a function of the Fe^{2+}/Fe^{3+} ratio, solids loading, pH, and aqueous Fe(II) concentration. Our results indicate that magnetite at the most favorable ratio ($x = Fe^{2+}/Fe^{3+} = 0.5$) are unreactive with PCE and TCE over 150 days. At pH values and Fe(II) concentrations where $Fe(OH)_2$ precipitation is expected, however, transformation of PCE and TCE is observed. Thus, our findings imply that magnetite may not be reactive enough to be a major contributor to abiotic natural attenuation of PCE and TCE alone, unless it is in the presence of $Fe(OH)_2$.

TABLE OF CONTENTS

LIST OF TABLES

LIST OF FIGURES

CHAPTER I

INTRODUCTION AND LITERATURE REVIEW

Humans have altered biogeochemistry by releasing millions of tons of synthetic organic compounds into the environment (Taniguchi 2011; Barnes et al. 2008). As a result, tens of thousands of land masses and water bodies, are polluted with toxic substances from decades of human activities (Kueper et al. 2014; Gupta, Van Houtven, and Cropper 1996; Zogorski et al. 2006; Squillace et al. 1999; Cassman, Dobermann, and Walters 2002). World population growth continues to influence these changes in land-use and management that are shown to impact subsurface soils, sediments and groundwater environments (Taniguchi 2011). Investigating the geochemistry of altered subsurface environments and using our understanding of natural phenomena will assist in determining chemical pathways for element and nutrient cycling, assist with the development of predictive tools, and strategies for subsurface contaminant remediation (Borch et al. 2009; He et al. 2015).

In the early 1900s, the United States organic chemical industry experienced steady growth that led to the production of different solvents (Doherty 2000a, 2000b). The four most used chlorinated solvents for commercial and industrial purposes were carbon tetrachloride (CTC), 1,1,1-trichloroethane (TCA), tetrachloroethylene (PCE) also known as PERC and trichloroethylene (TCE). Of those four compounds, PCE and TCE production rates were as high as 700 million pounds per year by 1970, not including *1,1*-DCE, *cis*-DCE and *trans*-DCE as synthesis by-products (**Figure 1)**. tetrachloroethylene (PCE) and trichloroethylene (TCE), were used at thousands of industrial and commercial facilities as metal degreasing solvents and are

currently the preferred spotting agents at dry-cleaning facilities in the United States (Doherty 2000a, 2000b).

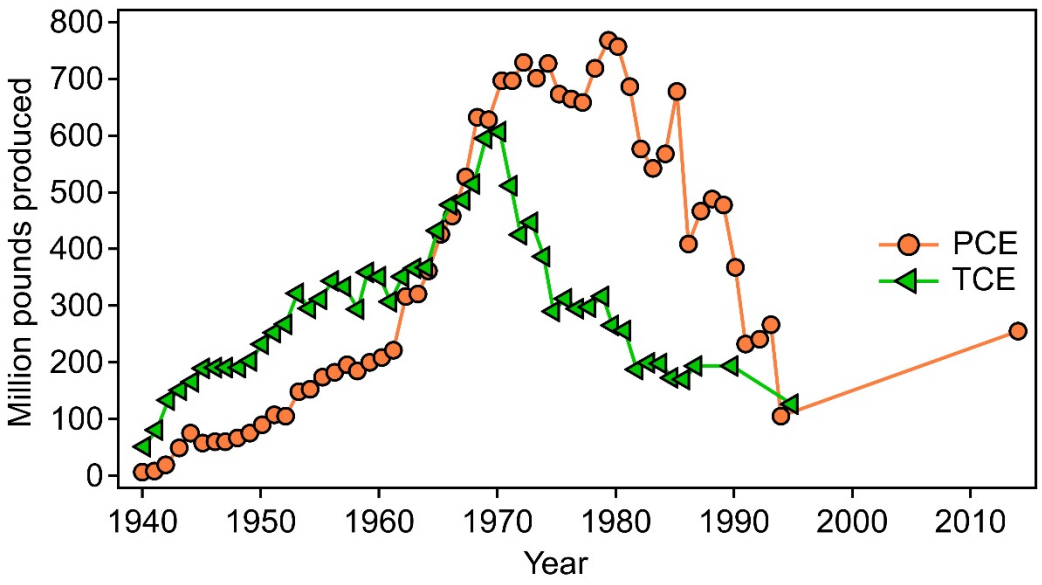

Figure 1. United States production of trichloroethylene (TCE) and tetrachloroethylene (PCE) (adapted from (Doherty 2000a, 2000b)).

Extensive poor handling, storage and waste disposal of these volatile organic solvents and by-products steered inadvertent environmental releases where tons of toxic chemicals leached through soils and entered hundreds of groundwater aquifers (Pankow and Cherry 1996; Kueper et al. 2014). Despite extensive remediation efforts, PCE and TCE are still detected at many groundwater sites above regulatory standards (**Figure 2)** (Kueper et al. 2014; Zogorski et al. 2006). For decades, PCE and TCE groundwater contaminants have been, and continue to be, a major concern for the environment and human health exposure (Guyton et al. 2014; Chiu et al. 2013). Today, PCE and TCE are two of the most frequently detected groundwater plume contaminants for both oxic and anoxic aquifers (Hawley, Deeb, and Levine 2014; Zogorski et al. 2006). Their carbon oxidation states range from +1 to +2. PCE and TCE are volatile, hydrophobic

and denser than water which are physical and chemical properties that influence their recalcitrance from biotic and abiotic degradation in the environment (McCarty, Stroo, and Ward 2010; Cwiertny and Scherer 2010).

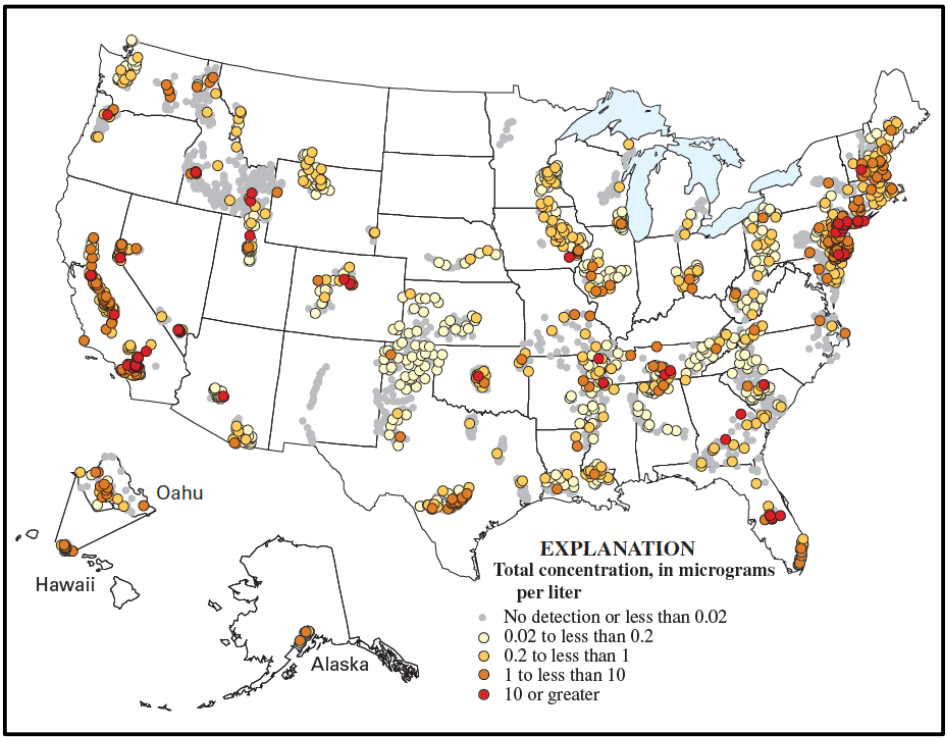

Figure 2. Volatile organic contaminant VOC contamination of groundwater aquifers throughout United States with a large range of detected concentrations (Zogorski et al. 2006).

The default groundwater treatment and plume containment approach has been pump and treat (Kueper et al. 2014). However, groundwater scientists have long projected that even with continuous pumping it would take more than several decades to reduce concentrations by a factor of 100 at tested superfund sites (Travis and Doty 1990). Therefore, the Department of Defense (DoD) reached a similar consensus after conducting a 15-year study that confirmed pump and treat

was costly and ineffective at remediating chlorinated ethenes from aquifers to regulated concentrations, or even site specific goals (Kueper et al. 2014).

Natural systems can be altered by microorganisms to reducing environments using elemental sulfur S^o, sulfate SO_4^{2-} and ferric iron Fe(III) as electron accepters (Weber, Achenbach, and Coates 2006; Madigan et al. 2010). Therefore, dissimilatory iron or sulfate reducing bacteria in anoxic environments cause reduced, and mobile ions, ferrous Fe(II) and sulfide S(-II), to become available in groundwater and soil systems (Lovley et al. 1987; Nealson and Myers 1992; Pennisi 2002).

A recent review proposed the degradation trend for chlorinated solvents with iron bearing minerals: disordered mackinawite FeS > FeS > Fe(0) > FeS_2 > sorbed Fe^{2+} > green rust = magnetite (Fe_3O_4) > biotite = vermiculite (He et al. 2015). From this group of iron materials, magnetite Fe_3O_4 as a reduced aquifer mineral is of great interests. Several reasons for interest with magnetite are due to microorganisms being able to biomineralize iron-bearing minerals, such as magnetite Fe_3O_4(s) (Bazylinski et al. 1995; Bazylinski, Frankel, and Konhauser 2007; Chang et al. 1989). The formation of magnetite also occurs through different abiotic processes (Gorski et al. 2010; Gorski and Scherer 2011a; Gorski and Fantle 2017) and magnetite is a mixed valent state iron oxide with different particle stoichiometries (x = Fe^{2+}/Fe^{3+} structural ratio) that range from oxidized x = 0 to stoichiometric x = 0.5, its fully reduced state. Other studies have shown stoichiometric magnetite drastically influenced the extent of contaminant reduction up to five-orders of magnitude (Gorski and Scherer 2009a; Latta et al. 2012). But the solid-state mineral stoichiometry of magnetite has not been monitored for experiments involving the reduction of chlorinated ethenes (Lee and Batchelor 2002a; Liang, Philp, and Butler 2009a; Sivavec 1998).

Like other iron oxides magnetite is ubiquitous and we know that it can form because of uniquely different chemical processes, for instance as aqueous Fe^{2+} catalyzed mineral recrystallization of ferrihydrite, lepidocrocite and goethite (Gorski et al. 2010; Gorski and Scherer 2011a; Hansel et al. 2003; Hansel, Benner, and Fendorf 2005). Available iron oxides with reducing Fe^{2+} and reduced free ions interact chemically via redox mechanisms (Gorski and Scherer 2011a). Some redox processes that happen as either a single step or a series of steps are (i) sorption (Fe^{2+} cation surface complexes to the mineral) (ii) electron transfer (Sorption, proceeded by an oxidation and electron transfer from the attached Fe^{2+} to an Fe(III) atom in the oxide) (iii) atom exchange (After step (ii) the electron can escape the solid phase Fe(III) bearing oxide as aqueous Fe^{2+}). Reviews explaining these novel redox processes more explicitly are available (Gorski and Fantle 2017; Gorski and Scherer 2011b).While biological degradation of PCE and TCE has been studied in some detail (Bradley and Chapelle 1997; Lee, Odom, and Buchanan Jr 1998), there is still significant knowledge gaps in our understanding of how abiotic processes with iron minerals such as magnetite (Fe_3O_4) might contribute to the degradation of chlorinated ethenes, such as PCE and TCE (He et al. 2015; He et al. 2009).

Magnetite is a common solid phase iron bearing mineral found within iron-reducing aquifers, and has been proposed as an important catalyst to support reductive transformation of chlorinated ethenes (Wiedemeier et al. 2017; Ferrey et al. 2004b; Lee and Batchelor 2002a). In recent years, the implications of various iron oxides for reductive dechlorination has advanced through ongoing investigations with several natural and fortuitously formed minerals with the potential to be implemented in iron-based groundwater remediation technologies like monitored natural attenuation (He et al. 2015; Cundy, Hopkinson, and Whitby 2008; Zhang 2003). Although it has been long recognized that iron minerals play an important role in redox dechlorination of

chlorinated ethenes, performance has not always been predictable or reproducible at the field scale, or even at the more controlled laboratory scale.

Magnetite was identified in sediment samples of the Twin Cities Army Ammunition Plant (TCAAP) where biological reductive dechlorination did not remove *cis*-DCE and 1,1-DCE dichloroethenes from a groundwater plume (Ferrey et al. 2004a). Despite the known tendency of reductive dechlorination of chlorinated ethenes in the order of decreasing numbers of chlorides PCE > TCE > *cis*-DCE > VC (Vogel, Criddle, and McCarty 1987) (**Figure 3**), only a few laboratory studies attempted to provide some evidence for the higher chlorinated PCE and TCE degradation by magnetite (**Table 1)** (Sivavec 1998; Lee and Batchelor 2002a; Liang, Philp, and Butler 2009b). Although non-sequential degradation has been suggested due to experiments involving lessor chlorinated solvents i.e., *cis*-DCE reacted with magnetite, PCE and TCE plus magnetite experiments with results that confirm a non-sequential degradation pathway, and specific transformation products at varied geochemical conditions such as greater than circumneutral pH is lacking. The only transformation product identified from Lee and Batchelor (2002a) magnetite reactions with PCE and TCE was chloride (Cl^-).

There are different inconsistencies regarding the rates and extent of reduction from laboratory experiments with TCE and PCE by magnetite. For TCE reacted with magnetite reported rates of degradation that differ by three orders of magnitude (Lee and Batchelor 2002b; Liang, Philp, and Butler 2009a; Sivavec 1998) (**Table 1**). Ferrous iron Fe(II) can surface complex with magnetite and reduce it (Gorski and Scherer 2009a), but to our understanding there is only a single experiment with TCE reacting with aqueous Fe(II) reduced magnetite reported in the literature (Sivavec 1998). For their study, a half-life of approximately 14 days was reported, but the authors fail to provide a transformation product distribution.

Assessing product distribution is crucial for a sustainable technology to be evaluated for field implementation, since partial reductive dechlorination of PCE or TCE may lead to significant accumulation of more toxic compounds like, *cis*–dichloroethene (*cis*-DCE) or vinyl chloride (VC) (He et al. 2015). The suggested degradation pathway and products for chlorinated ethenes observed by abiotic degradation of reactive iron bearing minerals is provided **(Figure 3)**. Here reductive elimination and hydrogenolysis to a much lesser extent tends to be preferred degradation pathways for chlorinated ethenes by reactive iron minerals (He et al. 2015).

The overall objectives of this research were to determine whether magnetite reduces PCE and TCE, and provide insight as to what geochemical conditions are necessary for predicting when magnetite may be a viable alternative treatment at groundwater aquifers. We measured the reduction for both organic solvents, PCE and TCE, with magnetite over a range of geochemical conditions. To date, it is unknown what affects the variability of the reported rates of reactions. Therefore, we varied the following factors for a range of experiments: (i) particle stoichiometry, (ii) freeze-dried versus non-freeze dried mineral, (iii) pH, (ii) mineral mass loading, (iii) concentration of aqueous iron(II). We found that magnetite alone only slowly transforms TCE, and does not react with PCE. When amended with aqueous Fe(II), only at conditions where ferrous hydroxide $Fe(OH)_2$ (s) is present with magnetite this dictates whether both PCE and TCE would degrade. To our knowledge, this is the first study to show that precipitated $Fe(OH)_{2\ (S)}$ plus magnetite activates a novel mechanism for dechlorination for both PCE and TCE.

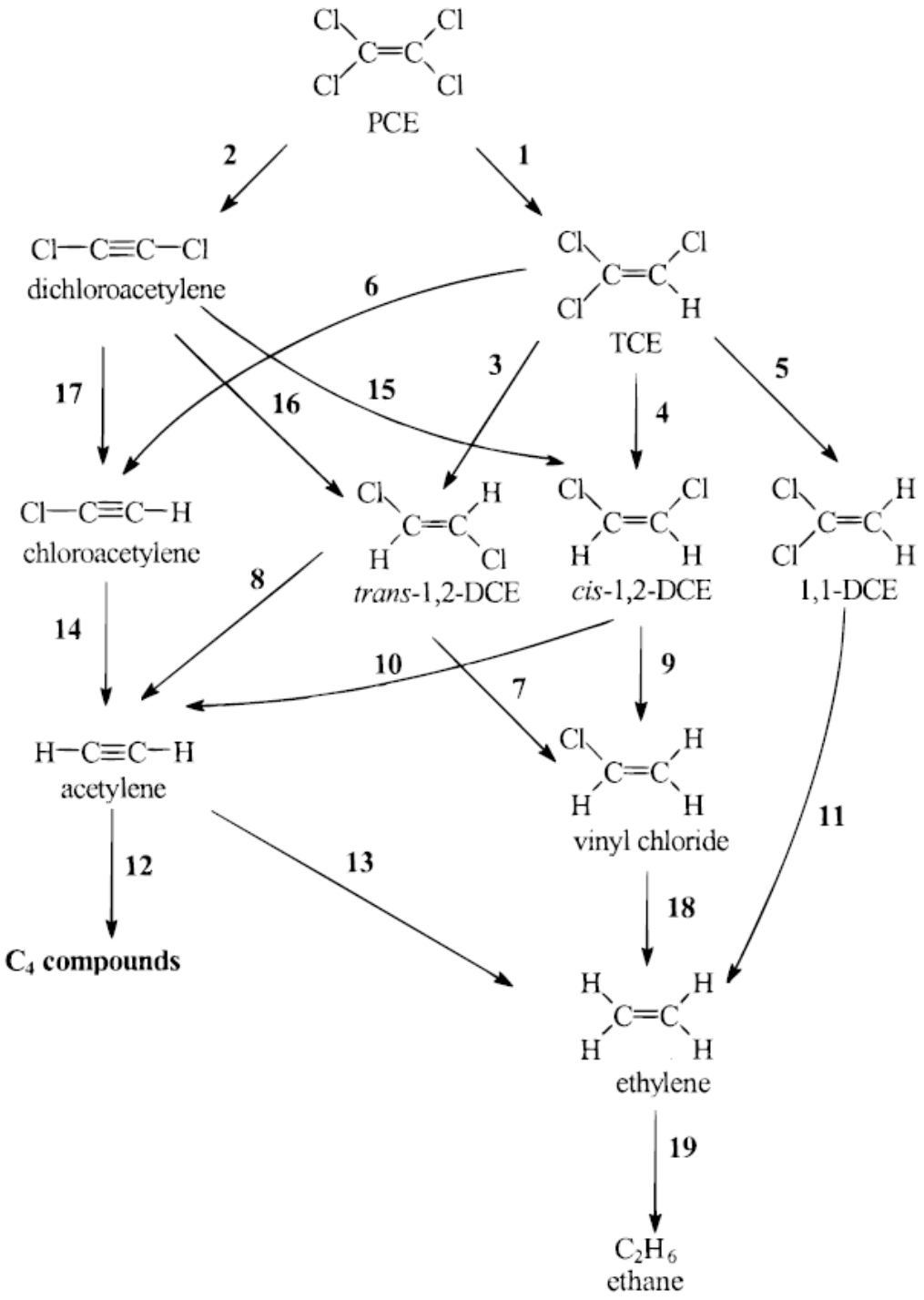

Figure 3. Summary of reaction degradation pathway for chlorinated ethenes during abiotic reduction by iron bearing minerals (Arnold and Roberts 2000; He et al. 2015).

Table 1. Literature Summary of Magnetite with TCE/PCE Kinetic Studies

Reactor type	$[C]_o$ µM	Mineral preparation	Conditions	Products %	% loss	k_{obs} Rate constant	References
			TCE				
[a]	-	-	81 m^2/L	-	-	4.3 x 10^{-7} s^{-1}	Sivavec et al. (1997)
[b,c] **Batch** 120 ml glass vial	7.3	-	pH 6.0 200 mM $FeSO_4$ in water	93.7	92.6	2.2 x 10^{-6} s^{-1}	Sivavec (1998)
Batch 20 ml glass vial	250	Precipitated and Freeze-dried	pH 7.0 3600 m^2/L 10 mM $NaHCO_3$	10.7	13.7	3.0 x 10^{-8} s^{-1}	Lee and Batchelor (2002)
[c] **Batch** 5 ml Flame sealed glass ampules	15	Precipitated based on Kang 1996 method	pH 8.0 1800 m^2/L 50 mM HEPES 0.06 M NaCl	2.9	7.14	6.5 x 10^{-9} s^{-1}	Liang and Butler et al. (2009)
			PCE				
Batch 20 ml glass vial	190	Precipitated and Freeze-dried	pH 7.0 3600 m^2/L 10 mM $NaHCO_3$	5.75	9.9	3.5 x 10^{-8} s^{-1}	Lee and Batchelor (2002)
[c] **Batch** 5 ml Flame sealed glass ampules	15	Precipitated based on Kang 1996 method	pH 8.0 1800 m^2/L 50 mM HEPES 0.06 M NaCl	10.8	23.1	1.5 x 10^{-8} s^{-1}	Liang and Butler et al. (2009)

[a] Mineral preparation and characterization approach not reported. [b] Dissolved Fe(II) amended reactions. [c] Trace detected products from noisy data, ≪ 10% initial mass. **$[C]_o$** The initial concentration of the TCE spiked within reactor. **(-)** Blank spaces are unreported information. Percent products and loss are given for the final time point reported.

CHAPTER II

MATERIALS AND METHODS

Chemicals

The target chlorinated analytes for this study were purchased from Sigma-Aldrich. The chemical grade of the Tetrachloroethylene (PCE) was anhydrous (≥ 99%) and Trichloroethylene (TCE) was reagent grade, ≥ 99%. The C2 expected daughter product gases were custom ordered from Praxair: as a 2.0% ethane, 1.97% ethylene and 1.9% acetylene mixture in nitrogen. Hexanes and methanol was also procured from Sigma-Aldrich and were pesticide residue grade and ACS reagent grade ≥ 99.8%, respectively. PCE and TCE (24, 250 & 500) mM stock solutions were gravimetrically prepared in N_2-sparged methanol, sealed with Viton septa and stored in a glovebox.

All deionized water was deoxygenated via nitrogen purging and allowed to sit for at least 24 hours within the glovebox before being used in any experiments. Either a 10 mM, 3-(N-Morpholino) propanesulfonic acid, 4 Morpholinepropanesulfoni acid MOPs titration grade (≥ 99.5%, Sigma) buffer solution or 10 mM Piperazine-N,N" – bis (3-propanesulfonic acid) PIPPs with a 10 mM sodium chloride NaCl background electrolyte was prepared as the aqueous phase for buffered controls and reactors (≤ pH 8.0 or ≥ 8.5), respectively. All pH adjustments were set with either degassed 5M hydrochloric acid (HCl) or (10 or 2.5M) sodium hydroxide (NaOH) ACS reagent grade (≥ 97.0%, Sigma).

Synthesis and Characterization of Minerals

Magnetite was synthesized using iron chloride salts following a method used as previously described (Gorski and Scherer 2010a). Briefly, 0.1 M Ferrous chloride ($FeCl_2$) and 0.2 M Ferric chloride ($FeCl_3$) solutions were prepared by dissolving the salts in deoxygenated deionized water in separate containers within the glovebox. Both solutions were combined then mixed with a magnetic stirrer. The mixture was vigorously stirred and titrated using 10M NaOH to set the pH within (10–11.5). The magnetite suspension was sealed and left stirring overnight before filtering. Freeze dried minerals, were ground in a porcelain mortar pestle, sieved through 150-micron sieve, and stored in the glovebox. With this approach the (~20 nm sphere) magnetite particles has surface area value close to 63 ± 7 m^2 g^{-1} using BET analysis (Gorski et al. 2009). Minerals were characterized with powder X-Ray diffraction (pXRD), 1,10 phenanthroline and Mössbauer spectroscopy (Gorski and Scherer 2010a). Post reacted minerals containing ferrous hydroxide was also characterized using pXRD. However, instead of mixing the material with glycerol to slow the rate of oxidation during characterization, we sealed the minerals with a single layer of kapton tape on a XRD slide. Electron microscopy was also used to confirm that the morphology and d-spacing of pre-reacted magnetite particles. A sample High resolution- transmission electron microscopy HRTEM using JEOL JEM 2100F is provided (**Figure 4)**. To prepare a microscopy sample, magnetite was suspended in methanol, then 30 µl drop was added to 2 mm carbon lacey copper grid. The methanol doused sample on the grid was left to evaporate in the glovebox before placing the TEM grid into a clean grid box in a desiccator before transportation to the instrument.

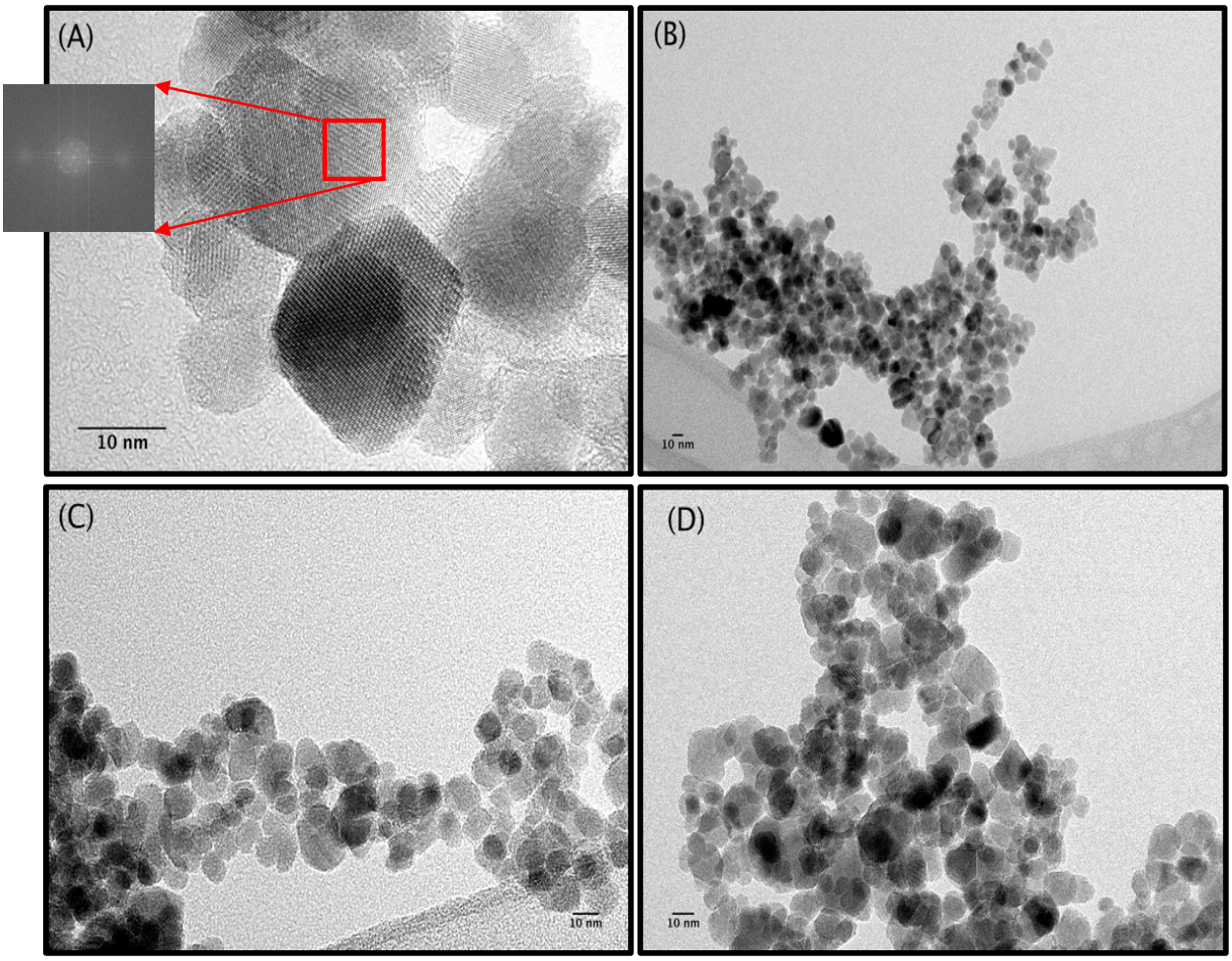

Figure 4. Sample HR-TEM images of pre-reacted Nano-magnetite (A – D). Miller indices and d-spacing (111) 0.46 nm/c, (311) 0.26 nm/c, (400) 0.21nm/c (A).

Sample Preparation and Stoichiometry Analysis

Magnetite stoichiometries (x= Fe^{2+}/Fe^{3+}) were determined using previously established methods (Gorski and Scherer 2010b). The first approach was stoichiometry from acid dissolution (x_d), were a target of 10 mM total iron in terms of magnetite mineral was dissolved in 5 M HCL under glovebox atmosphere. Using the phenanthroline method, we evaluated the Fe^{2+} and Total Fe concentrations to determine the stoichiometric ratio from a sample size of ten (n = 10). Powder X-ray diffraction (x_{xrd}) was the second approach, here we used a Rigaku MiniFlex II system equipped with a Co source (CoKα = 1.78899 Å). For pre-reacted magnetite, sample powders were mixed into two drops of glycerol to form a paste in the glovebox to avoid oxidation of the mineral during analysis. Samples were analyzed from 5-80^o 2θ with a 0.02^o step size and a 1.2 s dwell time. These pXRD stiochiometries (x_{xrd}) were then derived from a linear expression, evaluated from a observed trend where the unit-cell length was function of mineral stoichiometry (Gorski and Scherer 2010b). Transmission Mössbauer spectroscopy was performed with a variable temperature He-cooled system with a ^{57}Co source. To prepare samples and avoid oxidation, we sealed either powder or filtered specimens (with filter paper) between two pieces of kapton tape in the glovebox before mounting the sample unto the Mössbauer sample rod. To post characterize minerals using XRD, we shook the reactor, pull a ~5 ml sample and filtered the solution at the experiment's duration and sealed the sample with one layer of 25 μM kapton tape.

Reactor Design

All reactors were 160 ml glass bottles sealed with Viton septas (20 mm x 8 mm depth) and a 1:14 gas to liquid phase ratio. Each system was covered with foil, stored and shook at (~100 rpm) while upside down as shown in **figure 5**. The following parameters were varied within this study: magnetite stoichiometry (x = Fe^{2+}/Fe^{3+} structural ratio), solids loading, pH, and aqueous Fe(II) concentration. The desired mass of iron oxides was added to the buffer solution, followed by aqueous Fe(II), if needed. Then the reactor was pH adjusted and the target volume of chlorinated solvent spiked using a Hamilton syringe attached to a Chaney adaptor for studies requiring reproducibility. A PCE and TCE concentration of 50 µM (8,291 and 6,570 µg/L of PCE and TCE, respectively) was selected for most experiments, since it is an environmentally relevant value found at contaminated groundwater sites (Stroo et al. 2015; Kavanaugh, Deeb, and Hawley 2011; Ferrey et al. 2004b).

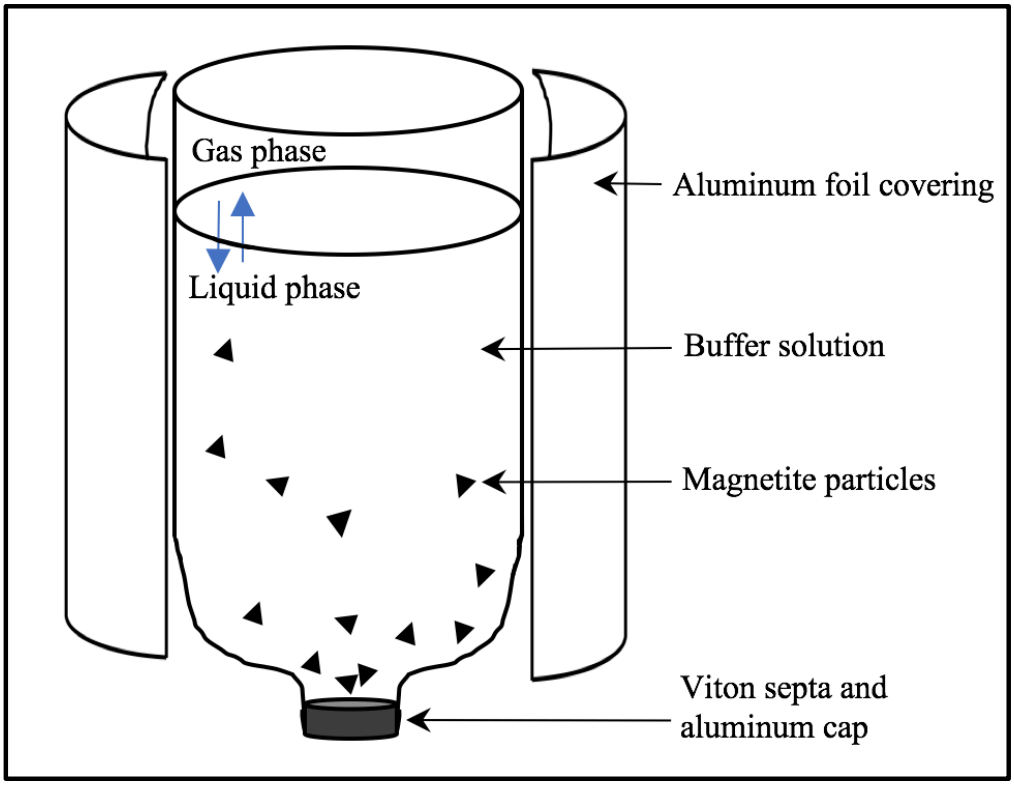

Figure 5. Schematic of the reactor design used for all experiments. Reactors was sealed in the glovebox, stored upside down on a shaker table at 100 rpm. Gas phase sampling was done with a nitrogen rinsed syringe. Liquid phase sampling was performed under glovebox atmosphere.

Analytical Procedures

All batch reactors were prepared in a 93% N_2/ 7% H_2 filled glovebox with an oxygen content maintained below 1 ppm. All reagents were degassed with nitrogen for 2 hours and left within the glovebox atmosphere for at least 24 hours to equilibrate. An Agilent 6890 gas chromatograph with electron capture (ECD) and flame ionization (FID) detectors was used to track parent and product analytes. A method developed for GC-ECD allowed for complete separation and detection of PCE and TCE using a Supelco Equity-5 column. All aqueous phase analytes were distinguished using GC-ECD Gas detector with an auto-sampler receiving 100 µl samples from GC vials. The aqueous sample was prepared using liquid-liquid extractions of 0.5 or 1 ml of sample to 2 ml of hexanes, vortexed and the supernatant transferred and sealed in GC vials. The ECD column was a Supelco Equity-5 DB-5, 250 µm i.d. x 30, with a 0.5 um film thickness, purchased from Sigma Aldrich. The carrier gas was nitrogen at a constant total flow velocities of 14.6 mL/min (10:1 split ratio). The detector make-up gas was 95% Argon: 5% methane with flow of 30 mL/min. The oven was programmed for an initial hold of 1 min at 45 ^{o}C, then 10 ^{o}C/min until all peaks were eluted or a temperature of 300 ^{o}C was reached. The ECD method detection limits are 0.05 µmoles/l PCE and 0.02 µmoles/l TCE for (n = 15).

The C2 daughter products ethane, ethylene and acetylene were detected using a GC-FID equipped with an Agilent J&W GC column, with a GS-GASPRO stationary phase, 0.320 mm i.d. x 30 m, under isothermal conditions at 70 °C. The carrier gas was nitrogen at a constant total flow velocitie of 14.1 mL/min (7.5:1 split ratio). The detector air flow was 450 mL/min, hydrogen flow 40 mL/min, and make-up gas type was nitrogen and a combined flow rate of 35 mL/min. The oven was programmed for an initial hold of 0.5 min at 70 ^{o}C, until a temperature of 260 ^{o}C was reached. All samples were 100 µl manual direct headspace injections into the column. The detection limits

for the FID method are 1.35 µmoles/l ethane, 1.36 µmoles/l ethylene and 1.34 µmoles/l acetylene for (n = 10).

To evaluate the partitioned phase for each analyte detected by the respective method, we used Henry's law and the specific dimensionless coefficient H^{cc} from a recent Henry's constants review (Sander 2015). The averaged values for the H^{cc} are as follows PCE = 1.54, TCE = 2.447, Ethane = 0.0471, and Ethylene = 0.146 and Acetylene = 1.016 (Sander 2015) (**Appendix**).

Reproducibility Experiment

A single set of data within this study was prepared with a sample size of twelve experiments with the following experimental condition (50 uM TCE, 5 g/L magnetite, 10 mM (558.5 mg/L) Fe(II) and pH 8.0). Four reactors were initially punctured, then unpunctured reactors were incrementally added within the sampling routine until the entire set of 12 reactors were sampled at the experiment duration.

Rate Constants

For each study, all observed first order rate constants (k_{obs}) were evaluated by negative natural logarithm of the ratio of final analyte concentration to initial concentration divided by the experiment duration.

RESULTS AND DISCUSSION

Reduction of PCE and TCE by Magnetite Alone

To evaluate the effect of magnetite stoichiometry on the reduction of TCE and PCE, we measured analyte concentration over time, as well as product formation in batch reactors. We first constrained our PCE and TCE reduction experiments over a range of environmentally relevant conditions including magnetite stoichiometries ($x = Fe^{2+}/Fe^{3+} = 0.48 – 0.5$), solids loadings (5 – 20 g/L), and pH values (7.0 – 9.4) **(Table 2, Figure 6).** We found no removal of both analytes over 140 days and detected no carbon products. The average carbon recovery was 101 ± 10% for ($n = 9$). Previous studies that reported TCE and PCE reduction by magnetite evaluated single geochemical conditions per report and when compared the results are inconsistent (**Table 1**). For TCE reactions with freeze dried magnetite, a degradation rate of $k = 4.3 \times 10^{-7}$ s^{-1} ($t_{1/2} = 0.052$ years) was reported without experimental conditions provided (Sivavec 1997). In a later study, it was shown that TCE with magnetite in batch at pH 7.0 was unreactive up to 14 days (Sivavec 1998). Recent batch experiments used ion and gas chromatography techniques on reactors with 63 g/L magnetite loading at pH 7.0. Using a chloride mass balance they found 11% total products transformation over 100 days and TCE degradation rate of $k = 3.0 \times 10^{-8}$ s^{-1} ($t_{1/2} = 0.73$ years) one order of magnitude slower than Sivavec's 1997 study (Lee and Batchelor 2002a). In addition, gas chromatography and isotope analysis methods were used with flame sealed glass ampules and 20 g/L magnetite loading at pH 8.0, which generated 3% transformation products over 131 days (Liang, Philp, and Butler 2009b). Since the collected data was relatively noisy, a degradation curve could not be explicitly assessed.

We also observed no loss of PCE or formation of products with magnetite suspensions over the similar conditions as our TCE reactors (**Figure 6**). These findings differed from the literature where it was shown that magnetite reduced 6% of the PCE added at pH 7.0 at a rate of k = 3.5 x 10^{-8} s^{-1} ($t_{1/2}$ = 0.63 years) (Lee and Batchelor 2002a). For a second study, approximately 11% products at pH 8.0 with 10% of the total mass was unaccounted (Lee and Batchelor 2002a; Liang, Philp, and Butler 2009b).

To investigate if freeze drying the magnetite particles influenced whether magnetite can reduce TCE, we prepared freshly precipitated magnetite and reacted it with TCE. Slow reduction of TCE was observed over 150 days with production of acetylene and trace ethylene and ethane (6% total products) (**Table 2, Figure 7**). The first-order rate coefficient of k = 2.9 x 10^{-9} s^{-1} ($t_{1/2}$ = 7.6 years) was estimated based on TCE removal. Based on these results, TCE reduction by freshly precipitated magnetite demonstrates for the first time that freeze drying affects the reactivity for magnetite minerals. Because of how slow the TCE reaction was we did not explore the reasons for differences in reaction for magnetite freeze dried versus nonfreeze dried. But similar results were found when working with freeze dried versus non-freeze dried iron sulfides (FeS) with TCE in batch experiments, where transformation kinetics with freeze-dried FeS was up to 20–50 times less reactive towards degrading TCE than non- freeze-dried FeS (He, Wilson, and Wilkin 2010). The authors suggest that freeze drying caused particle aggregation, decreased surface area and the availably of reactive sites. A second case showed that non-freeze dried suspensions are the only form of mackinawite that degrades *cis*-DCE, suggesting that this phenomena occurs with other iron minerals and even lesser chlorinated ethenes (Hyun and Hayes 2015). Since PCE should be more susceptible to reductive dechlorination, we hypothesized that reacting freshly precipitated nonfreeze dried magnetite with PCE would produce faster degradation than that observed with

TCE, but we detected no transformation even when the estimated mass loading of magnetite or available reactive sites approximately were doubled for our PCE experiment (**Table 2, Figure 8**). We believe these results suggest that for minerals that were not freeze dried another factor other than the availability of surface sites dictates the observed increased reactivity.

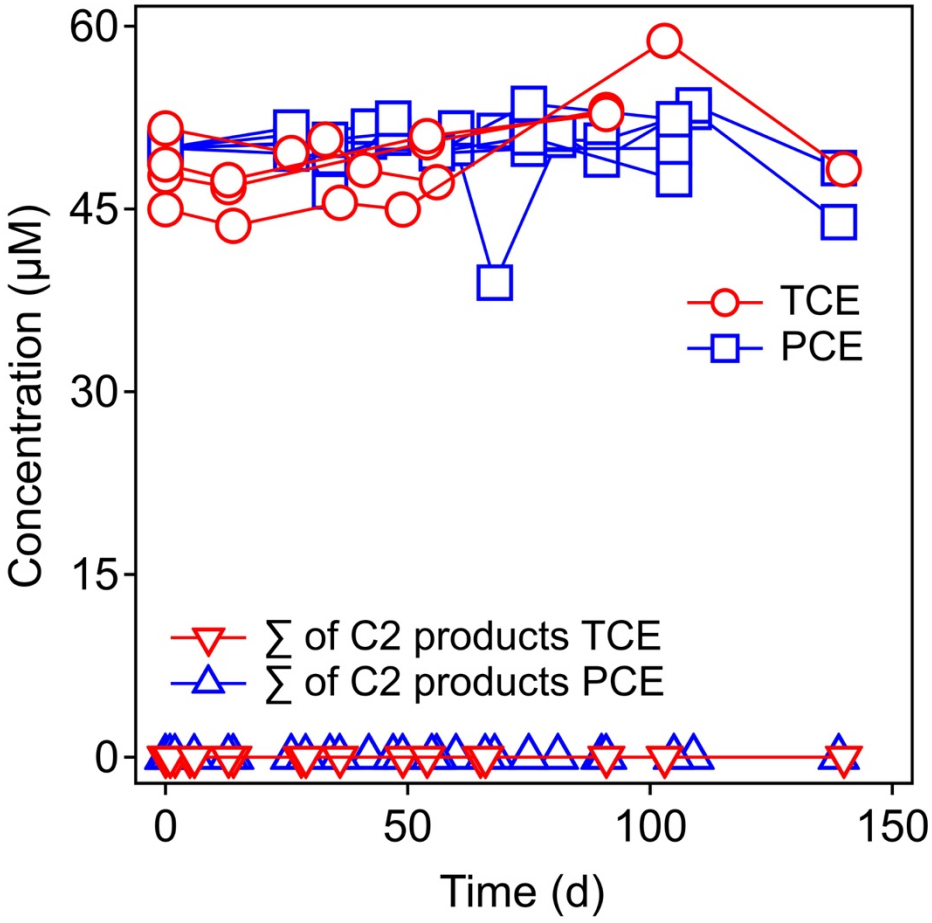

Figure 6. PCE and TCE concentration versus time in the presence of freeze dried magnetite. Experimental conditions: 50 μM PCE/TCE, 10 mM MOPs/NaCl at pH ≤ 8.0 or 10 mM PIPPs/NaCl at pH ≥ 8.5, pH range 7.0 – 9.4, magnetite stoichiometry (x_d= Fe^{2+}/Fe^{3+} = 0.48 – 0.55), mass loading 5-20 g/L. Average carbon recoveries, TCE (107 ± 8%) for (n = 4), and PCE (98 ± 6%), for (n = 5).

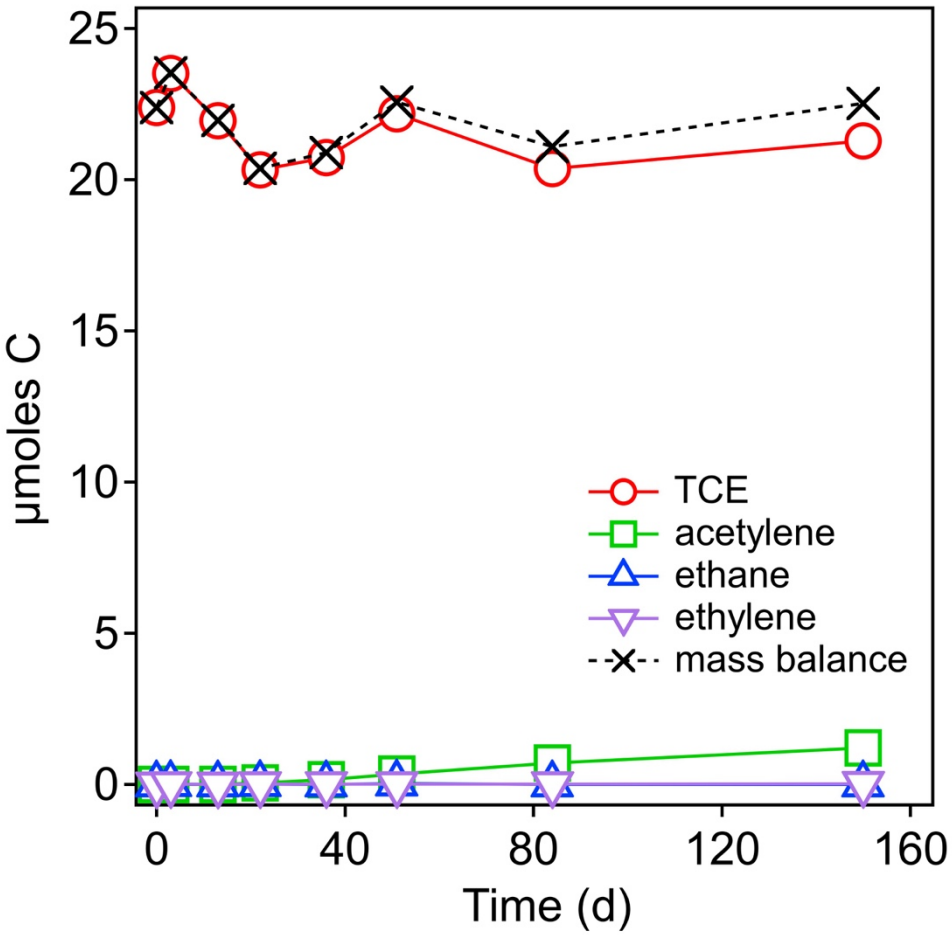

Figure 7. TCE concentration versus time in the presence of fresh magnetite. Experimental conditions: 73 µM TCE, 10 mM MOPs/NaCl, pH 8.0, magnetite stoichiometry (x_d= Fe^{2+}/Fe^{3+} = 0.48), mass loading 33 g/L.

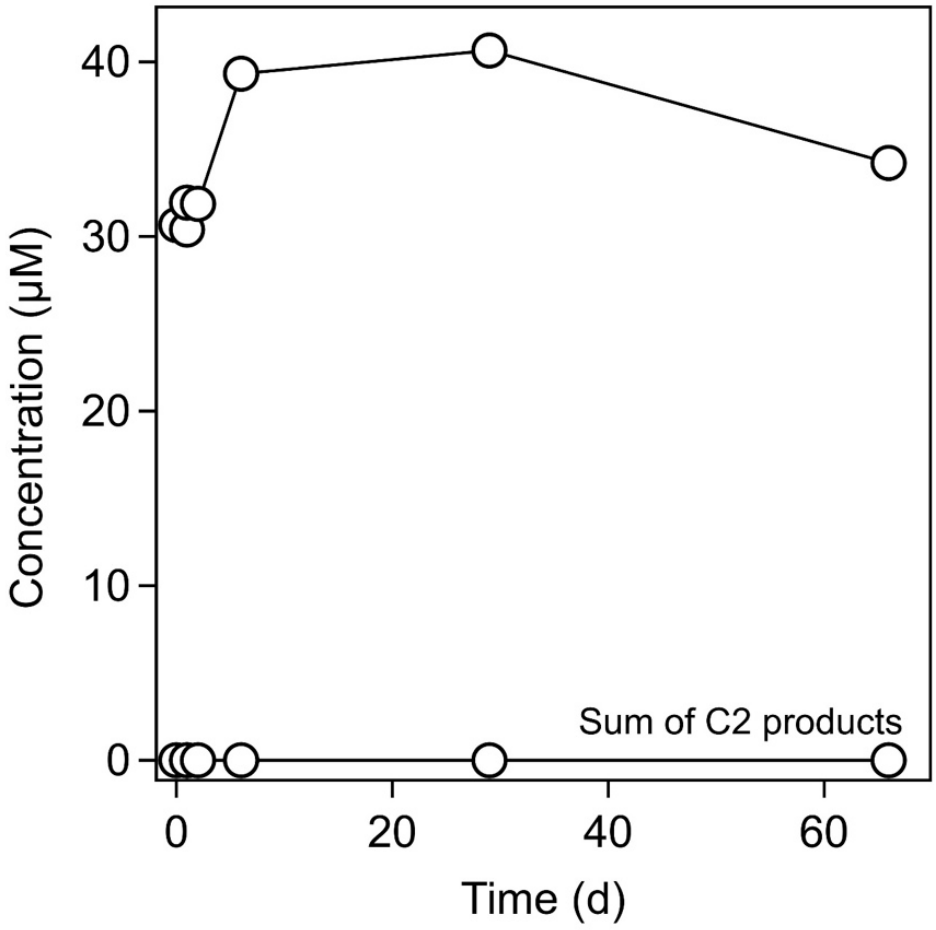

Figure 8. PCE concentration versus time in the presence of fresh magnetite. Experimental conditions: ~40 μM TCE, 10 mM MOPs/NaCl, pH 8.3, magnetite stoichiometry ($x_d = Fe^{2+}/Fe^{3+}$ = 0.5), mass loading 78 g/L.

Table 2. PCE/TCE with Magnetite alone

Exp. #	$[C]_o$ µM	pH	Mass Loading (g/L)	Stoichiometry x_{ms}	Stoichiometry x_d	Stoichiometry x_{XRD}	% loss	% Products	% C recovery	Duration (days)
					PCE					
1	~50	7.5	5	0.46	0.55 ± 0.02	0.53	7.0	0	88	139
2	~50	7.5	5	0.46	0.55 ± 0.02	0.53	7.0	0	97	139
3	~50	7.5	5	0.46	0.55 ± 0.02	0.53	6.9	0	101	105
4	~50	7.5	5	0.46	0.55 ± 0.02	0.53	6.87	0	96	105
5	~50	7.5	5	0.46	0.55 ± 0.02	0.53	6.87	0	106	105
*6	31	8.3	78	n.d.	0.5 ± 0.05	n.d.	-11.4	0	114	66
					TCE					
7	48	7.0	10	0.42	0.5 ± 0.02	n.d.	-10.7	0	111	91
8	52	7.5	5	0.46	0.55 ± 0.02	0.53	9.9	0	93	56
9	45	7.5	20	0.42	0.5 ± 0.02	n.d.	-6.3	0	106	140
10	49	8.0	10	0.42	0.5 ± 0.02	n.d.	-7.8	0	111	91
*11	50	7.8	68	n.d.	0.21 ± 0.008	0.21	-0.1	0	105	66
*12	58.7	7.9	72	n.d.	0.57 ± 0.013	0.52	8.0	0	95	65
*13	36	9.4	78	n.d.	n.d.	0.5	-14.9	0	118	66
**14	73	8	33	0.48	0.53	n.d.	5	6	101	150
**15	642	8	33	0.48	0.53	n.d.	8	0.22	92	150

(*) The magnetite mineral used in the reactor was freshly precipitated and not freeze dried. (**) means the same conditions of single star (*), but this time the particles were centrifuged, and re-suspended in buffer solution before added to the reactor. **$[C]_o$** is the initial concentration of the analyte spiked within reactor. % products and % analtye loss are at the final reported time point. **(~)** indicates that first time point determined was not at time zero. **(n.d.)** means a measurement not determined.

Reduction of PCE and TCE by Magnetite and Fe(II)

Although nonfreeze dried magnetite alone reduces TCE only slowly (and not PCE), previous work observed TCE reduction when aqueous Fe(II) was added to freeze-dried magnetite suspensions (Sivavec 1998). To investigate the influence of added Fe(II), we measured TCE and PCE reduction by magnetite with the added aqueous Fe(II) over a range of Fe(II) concentrations and pH values (**Tables 4 & 5**). TCE reduction was observed under some conditions, and was reproducible (**Table 4, Figure 9**). Here, a sample size of 12 TCE experiments with 5 g/L magnetite, 10 mM Fe(II) and pH 8.0 had acetylene as the primary transformation product with trace ethylene and ethane accounting for 24 ± 5.6% total products, and 99 ± 11% carbon recovery at the final time point. The first-order rate coefficient for this study was $k = 1.97 \times 10^{-8}$ s^{-1} ($t_{1/2}$ = 1.1 years). We found that the addition of ferrous iron also led to measurable PCE reduction $k = 1.62 \times 10^{-8}$ s^{-1} ($t_{1/2}$ = 1.3 years) (**Table 4, Figure 10**). Like our TCE with magnetite with aqueous Fe(II) experiments, we detected acetylene as the main product and trace ethylene and ethane. Although 20% of the carbon mass balance was not recovered, we tested for lesser chlorinated solvents, DCEs, and did not detect any. In fact, we found that under several Fe(II) concentrations (0.6 – 201 mM) and pH conditions (6.0-9.2), significant to no dechlorination of both TCE/PCE occurred and lower chlorinated products not detected.

During setting up reactors, we observed a white precipitate forming and it appeared to control whether we observed TCE and PCE degradation or not (**Figure 11**). Based on the experimental conditions and the presence of the precipitate, we hypothesized that ferrous hydroxide $Fe(OH)_2(s)$ was forming under select conditions that catalyzed measurable degradation of TCE and PCE. To confirm whether magnetite and ferrous hydroxide were the only mineral

phases present in the TCE reactors, we used XRD and Mössbauer spectroscopy to characterize the minerals phases for multiple reactors. All XRD diffraction patterns confirmed that ferrous hydroxide precipitates were present with the initially added magnetite, and a sample is shown in **figure 12**. This sample was taken at 167 days of reaction with 30% total degradation products and corresponds to Exp. 19 (**Table 4**). Similar XRD patterns were observed for PCE plus magnetite at conditions saturated for ferrous hydroxide.

Mössbauer spectra for samples were measured at 140K to identify magnetite, and additional iron phases (**Figure 13, Exp 35**). The Mössbauer spectrum reveals two sextets and a Fe(II) doublet. As expected, the sextet with the dominant spectral area (≈ 47%) had a center shift (CS) and hyperfine splitting (H) consistent with the $^{Oct}Fe^{2.5+}$ site in magnetite (**Table 3**). Likewise the second sextet had a spectral area of (≈ 23%) with a center shift (CS) and hyperfine splitting (H) consistent with the $^{Oct,Tet}Fe^{3+}$ site in magnetite. Using the spectral areas for these two sites, the post reacted magnetite mineral phase was stoichiometric x_{ms} = 0.5. The Fe(II) doublet in the Mössbauer spectra comprised of 30% of the total iron area was ferrous hydroxide as confirmed using XRD (**Figure 12**). For tested samples, the Fe(II) doublet had CS = 1.24 mm/s and a quadrupole splitting (QS) = 3.04 mm/s. No other mineral phases besides magnetite and ferrous hydroxide, were detected for reactors prepared with Fe(II) from ferrous chloride iron stock solutions.

To assess whether the ferrous hydroxide precipitate catalyzed the reduction of PCE and TCE, we plotted the initial conditions of all experiments on a $Fe(OH)_2(s)$ solubility diagram (**Tables 4 & 5, Figure 14**). For each solubility diagram in this study, red solid circle markers represent reactors that detected C2 transformation products (Acetylene, Ethene and Ethane), and yellow solid circle markers those with no degradation. A noticeable pattern of PCE and TCE

reduction occurs only when the experimental conditions are saturated for $Fe(OH)_2(s)$. Of the thirty-six experimental conditions investigated for, thirty (~83 %) experiments follow the pattern of TCE reduction being observed only when $Fe(OH)_2(s)$ solubility is exceeded (**Figure 14**). Only two out of thirty-six experiments were exceptions to this pattern when saturated for $Fe(OH)_2(s)$, and a single experiment with products when below $Fe(OH)_2(s)$ saturation (**Table 4, Exp 25**).

Similar experiments were conducted for PCE with magnetite and Fe(II) and like our TCE results, PCE reduction was favored once $Fe(OH)_2(s)$ precipitated (**Figure 14**). Of fifteen conditions evaluated, nine experiments were saturated for ferrous hydroxide and all had measurable transformation products. We explored whether non-freeze dried magnetite saturated for $Fe(OH)_2$ (s) may enhance the extent of degradation for TCE and PCE (Labeled with (**) on **Table 4**). As expected degradation occurred for TCE and PCE in freshly precipitated magnetite with $Fe(OH)_2(s)$ suspensions, but we found no evidence for increased rates of either TCE nor PCE degradation, when compared to reactions with freeze dried magnetite. We decided to repeat Sivavec's study using a similar mass loading of magnetite, the same very high concentration of aqueous iron at pH 6, and found completely no signs of degradation with almost complete mass recovery up to 100 days (**Table 5, yellow square** **Figure 15**).

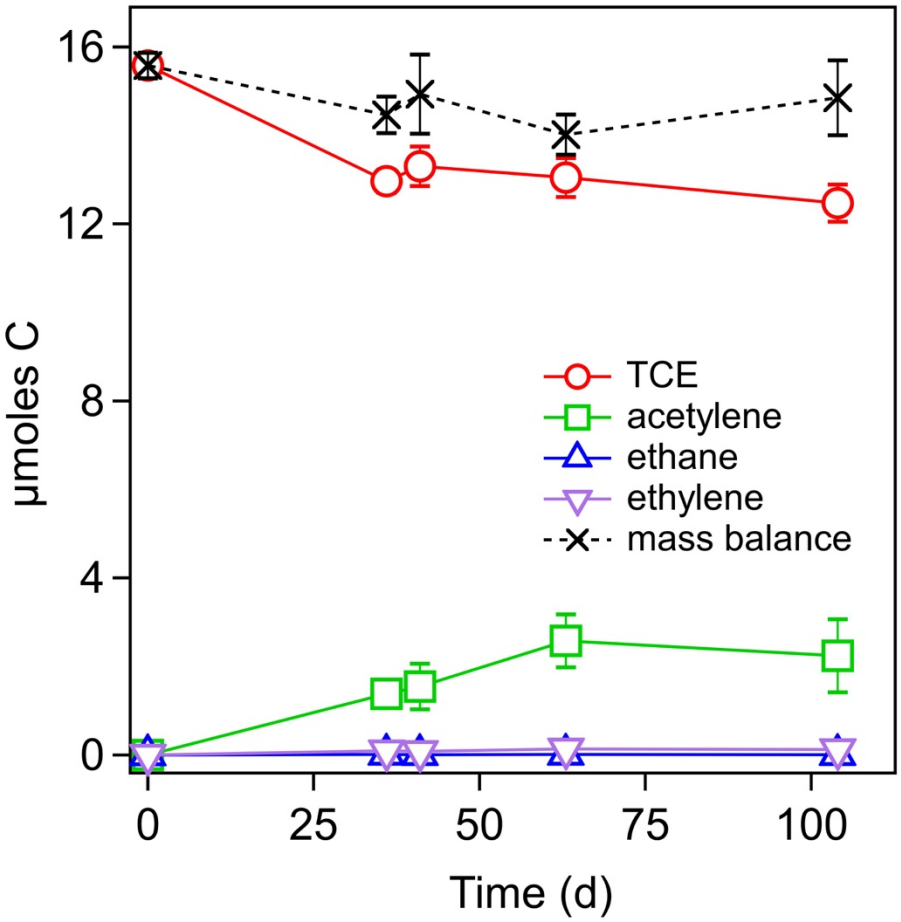

Figure 9. Reduction of TCE over time with freeze dried magnetite and aqueous Fe(II). Experimental conditions: 50 µM TCE, 5 g/L Fe3O4 (s), 9.3 ± 0.6 mM Fe(II), 10 mM MOPs/NaCl, pH 8, for (n = 12).

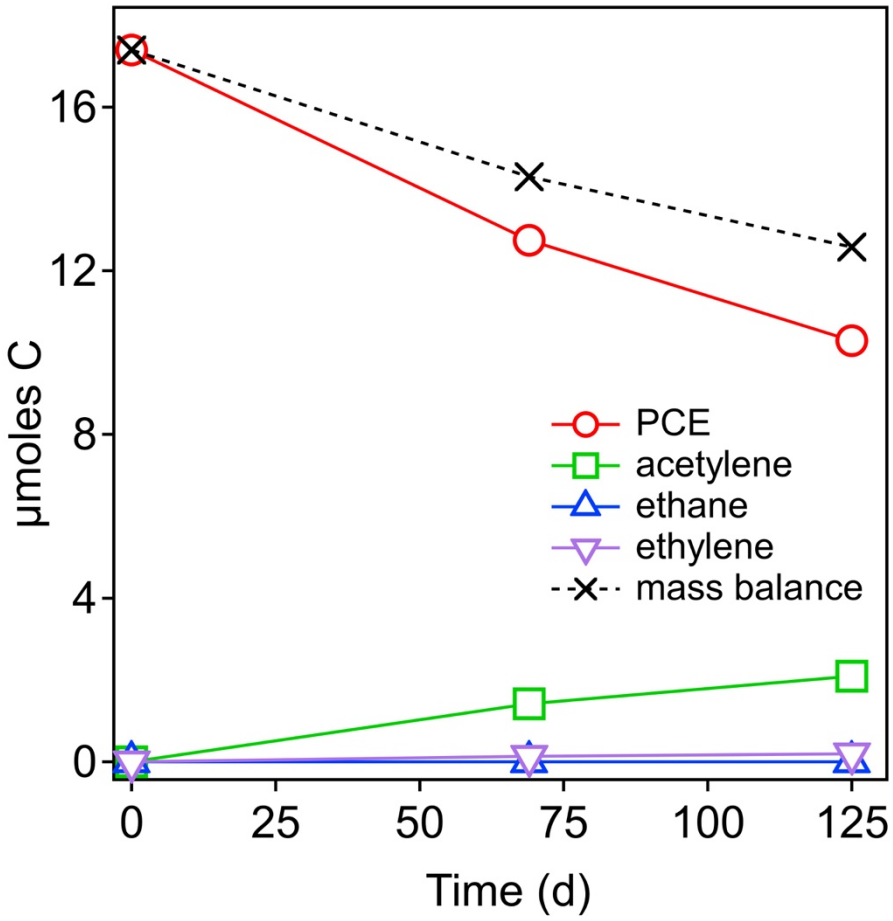

Figure 10. Reduction of PCE over time with freeze dried magnetite and aqueous Fe(II). Experimental conditions: 54 µM TCE, 5 g/L Fe3O4 (s), 33 mM Fe(II), 10 mM MOPs/NaCl, pH 7.9.

Figure 11. Images of 50 µM TCE reactors with low Fe(II) (Left reactor) and precipitated Fe(OH)2(s) (Right reactor) with 5 g/L magnetite in 10 mM MOPs buffer at pH 8.0.

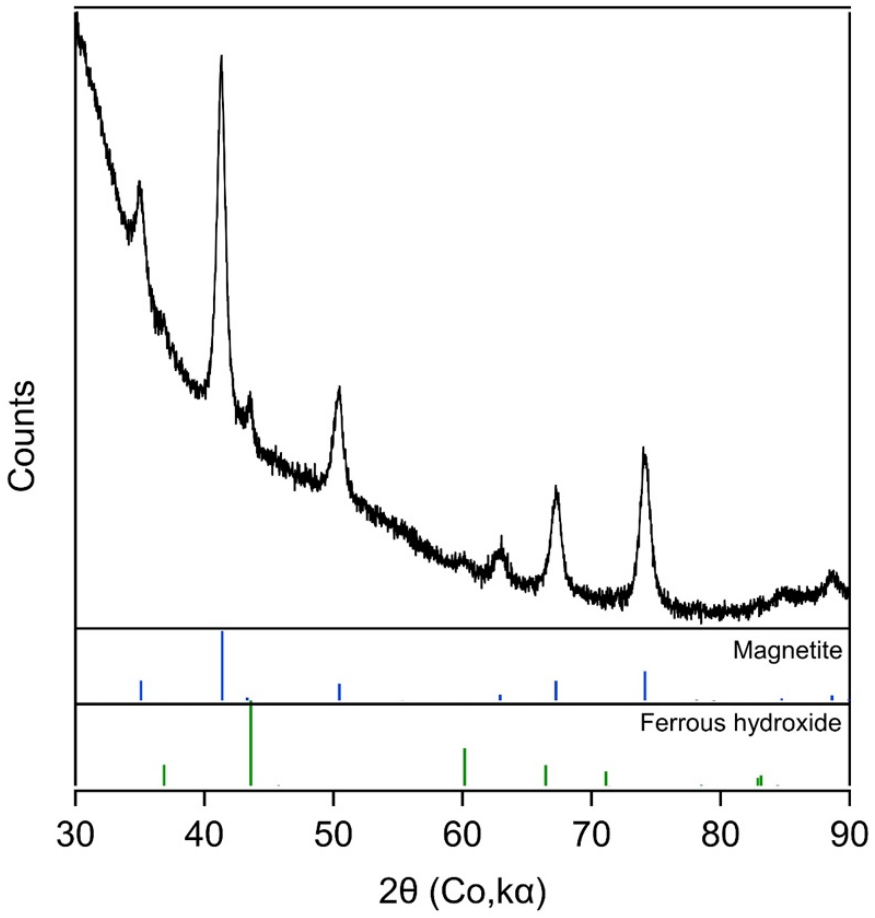

Figure 12. X-ray diffraction pattern of a TCE reactor with magnetite and Fe(II) where 30.0% products were observed. Light green bars indicate ferrous hydroxide and blue bars magnetite. Background prior 40 is due to kapton film used to seal the sample from being oxidized. Experimental conditions: 51µM TCE, 10 mM MOPs/NaCl, 9.2 mM Fe(II), pH 8.0.

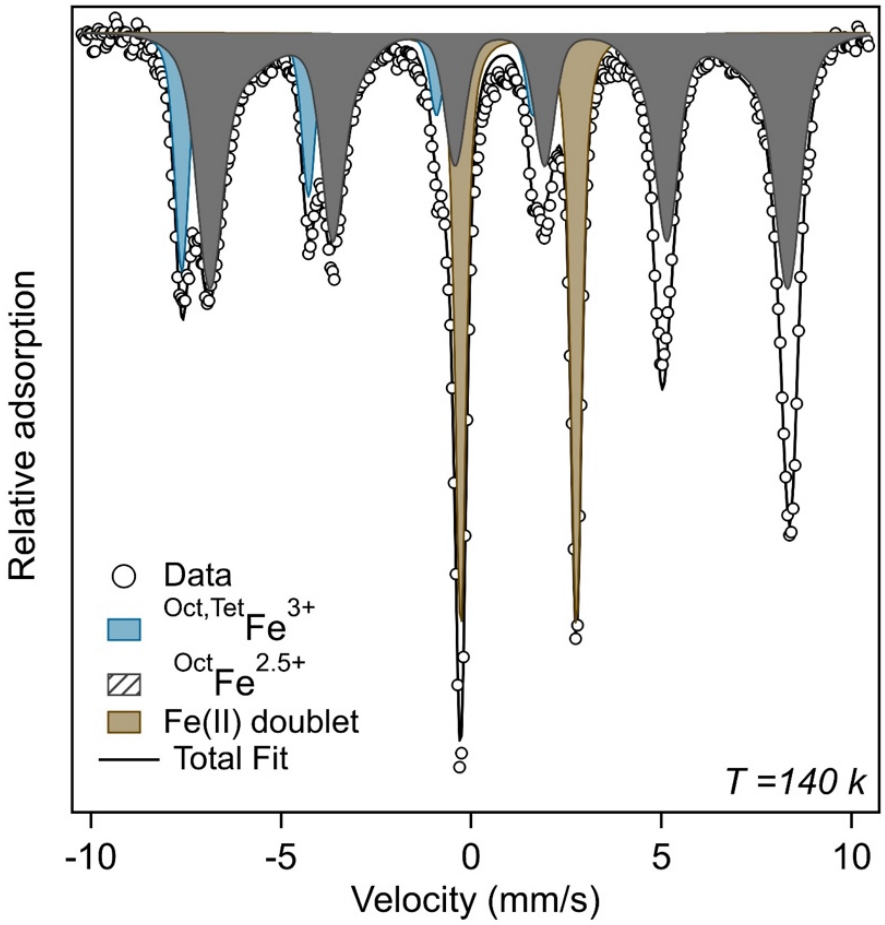

Figure 13. Mössbauer spectrum of magnetite plus ferrous hydroxide after reaction with 51 µM TCE, 10 mM MOPs/NaCl, pH 8.0. After 167 d, 30.0% total products were observed. Note: 9.2 mM Fe(II) was the initial concentration of dissolved iron added.

Table 3. Mössbauer Parameters for Magnetite, pre-and post reacted with Fe(II) and TCE

		$^{Oct}Fe^{2.5+}$				$^{Oct,Tet}Fe^{3+}$				Fe(II) doublet[a]			Magnetite stoichiometry		
Sample	Temp K	CS (mm s^{-1})	ε (mm s^{-1})	H (T)	Area (%)	CS (mm s^{-1})	ε (mm s^{-1})	H (T)	Area (%)	CS (mm s^{-1})	|Δ| (mm s^{-1})	Area (%)	x_{XRD}[b]	x_d[c]	x_{MS}[d]
Unreacted	140												0.48	0.53	
Exp. 34.	140	0.75	-0.02	46.1	46.8	0.37	0.01	49.4	23.3	1.24	3.04	29.9	-	-	0.50
Exp. 35	140	0.74	-0.01	46.0	52.5	0.37	0.02	49.6	23.5	1.24	3.04	24.0	-	-	0.53

[a] $Fe(OH)_2$ Fe identified by X-ray diffraction

[b] Magnetite x_{XRD} determined by X-ray diffraction

[c] Magnetite x_d determined by acid dissolution

[d] Magnetite $x_{MS} = ½ (^{Oct}Fe^{2.5+})/(1/2\ ^{Oct}Fe^{2.5+} + ^{Oct,Tet}Fe^{3+})$

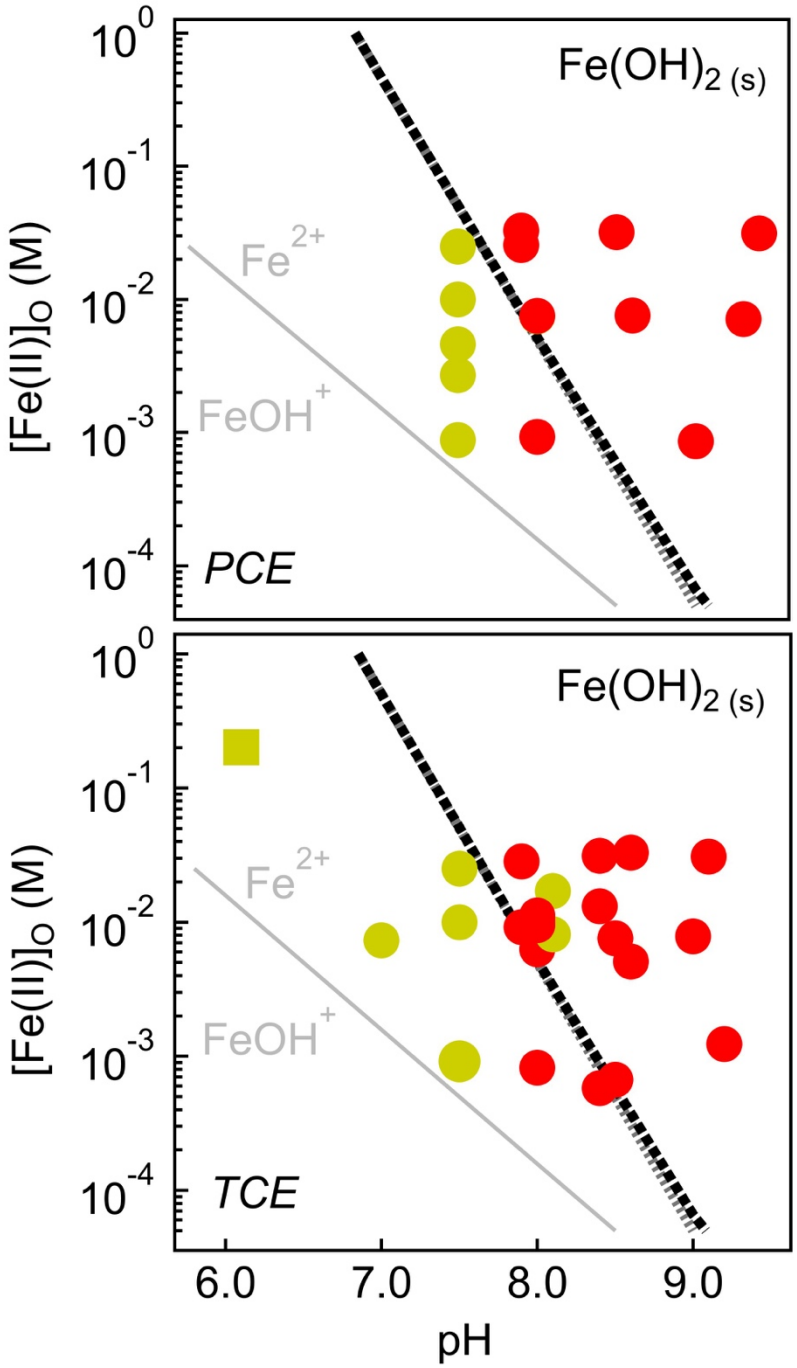

Figure 14. Fe(OH)2(s) solubility diagram with magnetite plus Fe(II) reactor conditions overlaid, (a) PCE and (b) TCE. Red markers represent PCE and TCE reactors with reduction products (acetylene, ethylene and trace ethane). Ksp $[Fe(OH)_2(s)] = [Fe^{2+}]\,[OH^-]^2 = 5 \times 10^{-15}$ M (Sawyer, McCarty, and Parkin 2016).

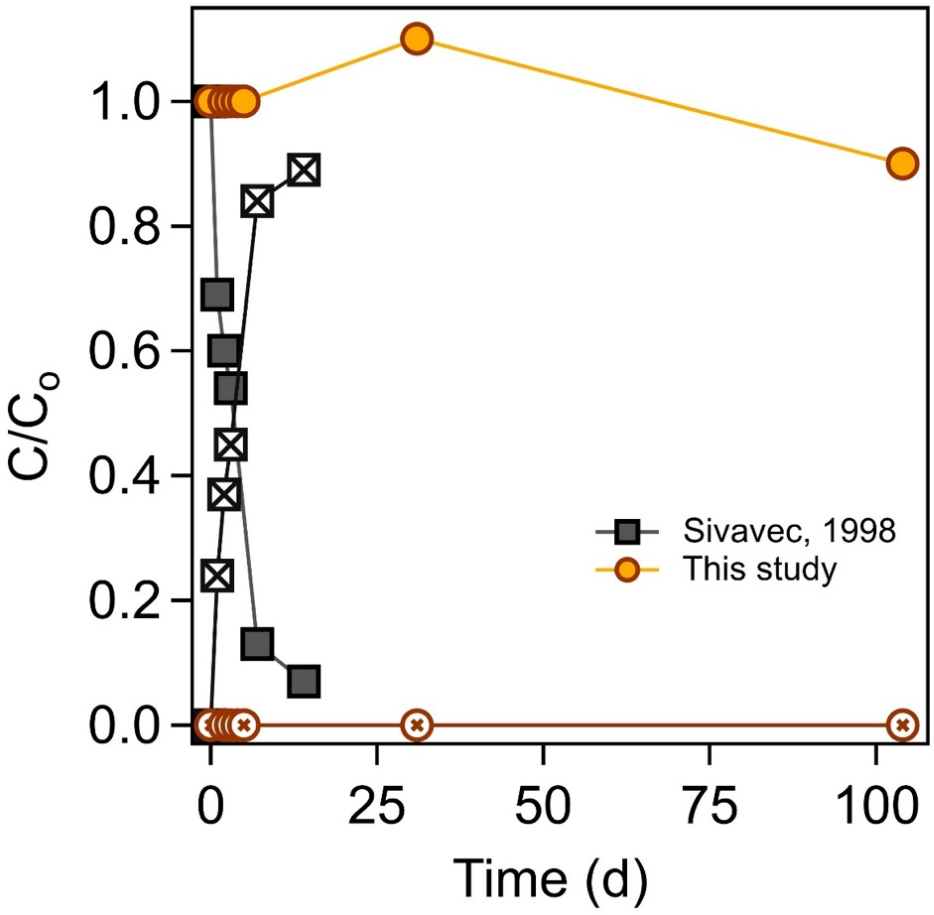

Figure 15. Reduction of TCE over time with freeze dried magnetite and aqueous Fe(II). Sivavec, 1998: 7.0 µM TCE, 217 g/L Fe3O4 (s), 200 mM Fe(II), pH 6.0. This study: 22 µM TCE, 147 g/L Fe3O4 (s), 201 ± 12 mM Fe(II), 10 mM MOPs/NaCl, pH 6.1.

Table 4. PCE/TCE Magnetite + aqueous Fe(II) reactors with products

Exp #	$[C]_o$ µM	pH	$[Fe(II)]_o$ mM	IAP/K_{SP}	$[Fe(II)]_f$ mM	$[Fe(II)]_{loss}$ mM	*k-obs* s^{-1}	Stoichiometry x_d	Stoichiometry x_{XRD}	Fe_3O_4 (g/L)	% loss	% Products	% C recovery	Duration (dy)
PCE														
**16	50.8	7.9	25.6	3.38	n.d.	n.d.	1.3×10^{-8}	0.80 ± 0.342	n.d.	≈ 7.0	8.8	1	93	82
17	53.7	7.9	32.9	4.55	29.7	-3.2	3.0×10^{-8}	0.52± 0.03	0.5	5.11	28	6	78	125
18	54.0	8.0	0.93	0.19	n.d.	n.d.	1.7×10^{-8}	0.54 ± 0.034	0.51	5	18	3	85	140
**19	57.7	8.0	7.54	1.51	n.d.	n.d.	2.5×10^{-8}	0.62 ± 0.07	n.d.	≈11	32	4	72	180
20	50.1	8.5	32.0	63.9	3.60	-28.4	4.9×10^{-8}	0.52± 0.03	0.5	5.11	40	16	76	125
21	55.3	8.6	7.58	20.0	1.61	-5.97	4.9×10^{-8}	0.52± 0.03	0.5	5.07	41	13	72	125
22	53.1	9.0	0.86	17.2	n.d.	n.d.	3.2×10^{-8}	0.54 ± 0.034	0.51	5	32	12	80	140
23	53.3	9.3	7.71	511	0.71	-7.0	3.6×10^{-8}	0.52± 0.03	0.5	5.03	32	10	77	125
24	45.8	9.4	31.4	4345	3.86	-27.54	4.9×10^{-8}	0.52± 0.03	0.5	5.03	41	15	74	125
TCE														
25	55.3	8.0	0.82	0.16	n.d.	n.d.	2.7×10^{-8}	0.54 ± 0.034	0.51	5	28	11	83	139
**26	76	8.0	6.30	1.26	n.d.	n.d.	3.0×10^{-8}	0.53	n.d.	33	33	22	90	150
**27	615	8.0	6.30	1.26	n.d.	n.d.	1.3×10^{-8}	0.53	n.d.	33	18	17	99	150
**28	52.4	8.0	7.44	1.49	n.d.	n.d.	1.4×10^{-8}	0.57 ± 0.024	n.d.	≈ 9.4	20	11	91	180
29	50.8	8.0	8.23	1.98	4.85	-3.38	1.9×10^{-8}	0.53 ± 0.013	0.48	5	24	24	99	167
30	51.6	8.0	8.54	2.05	4.23	-4.31	2.1×10^{-8}	0.53 ± 0.013	0.48	5	27	28	101	167
31	51.1	7.9	9.19	1.40	4.13	-5.06	2.0×10^{-8}	0.53 ± 0.013	0.48	5	26	18	93	167
32	50.5	8.0	9.19	1.84	5.09	-4.1	9.9×10^{-9}	0.53 ± 0.013	0.48	5	14	24	110	167
33	50.5	8.0	9.24	1.97	4.34	-3.87	2.5×10^{-8}	0.53 ± 0.013	0.48	5	31	30	99	167
34	50.5	8.0	9.24	1.85	5.2	-4.04	2.4×10^{-8}	0.53 ± 0.013	0.48	5	29	26	97	167
35	50.1	8.0	9.42	1.88	5.23	-4.19	2.2×10^{-8}	0.53 ± 0.013	0.48	5	28	30	102	167
36	49.8	8.0	9.49	1.90	5.48	-4.01	1.9×10^{-8}	0.53 ± 0.013	0.48	5	25	24	99	167
37	49.3	8.0	9.50	1.90	5.36	-4.14	1.7×10^{-8}	0.53 ± 0.013	0.48	5	22	24	102	167
38	50.5	8.0	9.52	1.90	4.98	-4.54	2.0×10^{-8}	0.53 ± 0.013	0.48	5	25	19	94	167
39	51.1	8.0	9.52	1.96	4.18	-5.34	1.9×10^{-8}	0.53 ± 0.013	0.48	5	24	20	97	167
40	54	8.0	10.0	2.0	n.d.	n.d.	9.4×10^{-8}	0.48 ± 0.03	0.56	5	75	46	71	168
41	51.2	8.0	10.69	2.57	4.57	-6.12	2.2×10^{-8}	0.53 ± 0.013	0.48	5	27	26	99	167
42	61.2	8.0	11.2	2.24	n.d.	n.d.	8.2×10^{-9}	0.48 ± 0.03	0.56	5	10	5	94	287
**43	50.4	8.0	29.4	6.15	n.d.	n.d.	6.9×10^{-9}	0.53 ± 0.045	n.d.	≈ 6.0	7	6	99	111
44	49.5	7.9	31.2	4.32	19.56	-11.64	1.2×10^{-9}	0.48± 0.03	0.45	5.03	-0.8	3	103	69
**45	53.7	8.4	0.58	0.64	n.d.	n.d.	3.9×10^{-9}	0.60 ± 0.038	n.d.	≈ 7.0	4	2	99	111
46	69.3	8.4	13.1	16.5	n.d.	n.d.	1.2×10^{-8}	0.48 ± 0.03	0.56	5	22	5	83	287
47	53.9	8.5	0.67	1.34	n.d.	n.d.	3.0×10^{-8}	0.54 ± 0.03	0.51	5	25	11	85	139
48	51.1	8.5	7.55	15.10	4.18	-3.37	4.5×10^{-9}	0.48± 0.03	0.45	4.97	5	2	97	125
**49	55.9	8.6	5.09	12.8	n.d.	n.d.	1.9×10^{-8}	0.66 ± 0.01	n.d.	≈ 7.0	17	12	95	111
50	51.5	8.6	32.9	86.6	3.50	-29.4	4.1×10^{-9}	0.48± 0.03	0.45	5.03	4.5	4	99	125
51	54.2	9.0	7.83	172	0.58	-7.25	1.3×10^{-8}	0.48± 0.03	0.45	5.03	13	3	90	125
52	52.2	9.1	30.9	1177	1.87	-29.03	1.0×10^{-8}	0.48± 0.03	0.45	5.01	11	4	93	125
**53	53.7	9.2	1.23	67.6	n.d.	n.d.	1.3×10^{-8}	0.59 ± 0.013	n.d.	≈ 16.0	12	4	92	110

(*) The magnetite Fe_3O_4 mineral used in the reactor was freshly precipitated and not freeze dried. (**) means the same conditions of single star (*), but this time the particles were centrifuged, and re-suspended in buffer solution before added to the reactor. **$[C]_o$** is the initial concentration of the analyte spiked within reactor. **[Fe(II)]** Iron concentration with subscript (**o, f** and **loss)** means the initial, final dissolved iron concentration and the difference of the final from the initial concentrations respectively. Percent products, TCE loss and carbon recovery at the final reported time point. **(~)** First time point determined was not at time zero. **(n.d.)** indicates not determined. Reactors were set-up using 10 mM MOPs / NaCl or 10 mM PIPPs / NaCl buffers originally set at pH 7.0 and 8.5, respectively. MOPs buffer was used to set up all reactors ≤ 8.0, and PIPPs for reactors within the range of (8.5 – 9.0). **% analtye loss, % Products** and **% Carbon recovery** are taken from the final reported time point. **Bolded** rows are used for reactors that a white cloudy precipitate was observed. The ion activity product (**IAP**) was determined with initial conditions for each experiment. **IAP/K_{sp}** values at equilibrium indicates the following w/ respects to potential ferrous hydroxide $Fe(OH)_2$ formation, **< 1 undersaturated, = 1 saturated, > 1 supersaturated** for a $K_{sp} = [Fe^{2+}] [OH^-]^2 = 5 * 10^{-15}$ mM and IAP determined from experimental **pH** and **$[Fe(II)]_o$** values.

Table 5. PCE/TCE with Magnetite + aqueous Fe(II) reactors without products

Exp #	$[C]_o$ µM	pH	$[Fe(II)]_o$ mM	IAP/K_{SP}	$[Fe(II)]_f$ mM	$[Fe(II)]_{loss}$ mM	k_{obs} s^{-1}	Stoichiometry x_d	Stoichiometry x_{XRD}	Fe_3O_4 (g/L)	% loss	% Products	% C recovery	Duration (dy)
PCE														
54	~50	7.5	2.7	0.05	n.d.	n.d.	0	0.55 ± 0.02	0.53	5	10	0	90	78
55	~50	7.5	4.6	0.09	n.d.	n.d.	0	0.39 ± 0.03	0.54	5	2.8	0	97	78
56	65	7.5	10.0	0.20	n.d.	n.d.	0	0.50 ± 0.06	n.d.	17	-24.5	0	125	91
57	~70	7.5	25.0	0.50	n.d.	n.d.	0	0.50 ± 0.06	n.d.	17	-14.5	0	115	91
58	48.9	8.0	7.47	1.64	7.13	-0.34	0	0.52± 0.03	0.5	5.07	6.4	0	96	125
59	51.7	7.5	0.88	0.018	n.d.	n.d.	0	0.54 ± 0.034	0.51	5	26	0	74	140
TCE														
‡60	22	6.1	201	0.01	n.d.	n.d.	0	0.43	n.d.	147	3.8	0	96	104
**61	54.3	7.0	7.73	0.02	n.d.	n.d.	0	n.d.	n.d.	≈15.0	5	0	95	55
62	51	7.5	10.0	0.20	n.d.	n.d.	0	0.50 ± 0.06	n.d.	20	4.0	0	96	128
63	50.5	7.5	25.0	0.50	n.d.	n.d.	0	0.50 ± 0.06	n.d.	20	-2.0	0	102	128
*64	54.7	8.1	17.0	5.39	n.d.	n.d.	0	0.56 ± 0.04	0.43	68	-0.3	0	103	66
65	55.2	8.1	8.11	2.82	7.25	-0.86	0	0.48± 0.03	0.45	5.01	6	0	94	195
66	55.9	7.5	0.92	0.02	n.d.	n.d.	0	0.54 ± 0.034	0.51	5	26	0	74	139

(*) The magnetite Fe_3O_4 mineral used in the reactor was freshly precipitated and not freeze dried. (**) means the same conditions of single star (*), but this time the particles were centrifuged, and re-suspended in buffer solution before added to the reactor. **$[C]_o$** is the initial concentration of the analyte spiked within reactor. **[Fe(II)]** Iron concentration with subscript (**o, f** and **loss)** means the initial, final dissolved iron concentration and the difference of the final from the initial concentrations respectively. Percent products, TCE loss and carbon recovery at the final reported time point. **(~)** First time point determined was not at time zero. **(n.d.)** indicates not determined. (‡) 22 g of a mixture of freeze dried magnetite stoichiometry determined by a weighted average. Reactors were set-up using 10 mM MOPs / NaCl or 10 mM PIPPs / NaCl buffers originally set at pH 7.0 and 8.5, respectively. MOPs buffer was used to set up all reactors ≤ 8.0, and PIPPs for reactors within the range of (8.5 – 9.0). **% analtye loss, % Products** and **% Carbon recovery** are taken from the final reported time point. **Bolded** rows are used for reactors that a white cloudy precipitate was observed. The ion activity product (**IAP**) was determined with initial conditions for each experiment. **IAP/K_{sp}** values at equilibrium indicates the following w/ respects to potential Ferrous Hydroxide $Fe(OH)_2$ formation, **< 1 undersaturated, = 1 saturated, > 1 supersaturated** for a $K_{sp} = [Fe^{2+}][OH^-]^2 = 5 * 10^{-15}$ mM and IAP determined from experimental **pH** and **$[Fe(II)]_o$** values.

Reduction of PCE and TCE by Ferrous hydroxide

The observation of $Fe(OH)_2(s)$ precipitation being necessary for PCE and TCE reduction to occur, however, begs the question of whether $Fe(OH)_2(s)$ alone or even aqueous Fe(II) alone can reduce TCE, or whether magnetite needs to be present for TCE reduction to occur. To evaluate whether $Fe(OH)_2(s)$ alone or aqueous Fe(II) alone could reduce TCE, we measured TCE reduction over a range of Fe(II) concentrations and pH values and plotted the results on an $Fe(OH)_2(s)$ solubility diagram (**Table 6, Figure 16**). As expected, no reduction of TCE was observed by aqueous Fe(II). Interestingly an even more selective degradation trend is noticeable rather than the trend observed for magnetite plus Fe(II) experiments. Here, TCE reduction was measured when $Fe(OH)_2(s)$ has also precipitated, but the initial Fe(II) concentration must surpass 13 mM (**Figure 16**). The average percent carbon mass recovery was 95 ± 30% for (n = 8). We prepared PCE plus aqueous Fe(II) reactors with an Fe(II) range of (0.30 to 32) mM and pH range from 7.0 thru 9.2 (**Table 6, Figure 16**). Like our TCE experiments, PCE removal only occurred when $Fe(OH)_2(s)$ was present from an initial Fe(II) concentration greater than 13 mM. A qualitative assessment remarkably confirm that the appearance or absence of the white precipitate closely followed the solubility of ferrous hydroxide (**Figure 17)**.

To confirm that the reactive solid phase was solely ferrous hydroxide, we characterized the solid materials in our reactors after ~150 days reaction using powder X-ray diffraction (pXRD) and Mössbauer spectroscopy. Both pXRD and Mössbauer confirmed that the mineral phase in these reactors was $Fe(OH)_2$ (s) (**Figures 18-19**). Although we observed some black and bluish gray specks in some reactors where transformation of TCE and PCE occurred, the total mass of these solid phases was less than ~ 2% of detection limits for both Mössbauer spectroscopy and pXRD.

As expected, the Mössbauer spectrum of the post reacted $Fe(OH)_2$(s) sample at 140 K contains a single Fe(II) doublet, and a negligible amount of ferric iron Fe(III) (**Figure 20**). We ran the samples at 13 K, where the $Fe(OH)_2$ spectrum is an octet with parameters that are similar to those published for ferrous hydroxide (**Figure 16**) (Miyamoto, Shinjo, and Takada 1967; Genin et al. 1986). Ferrous hydroxide undergoes antiferromagnetic ordering below its Néel temperature of ~30 K, which results in the ferrous octet spectra as determined from our results.

To explore differences in kinetics of abiotic reduction of TCE by magnetite plus ferrous hydroxide versus ferrous hydroxide alone, the results are summarized in **figure 20,** by plotting experiments at 10 mM Fe(II) at pH 8.0, and 30 mM at pH 8.5 – 9.0. Gray closed markers are the sum of products for reactors with magnetite, and the blue open markers indicate products because of ferrous hydroxide. At the 30 mM Fe(II) pH 8.5 and 9.0 conditions, we observed that the presence of magnetite does not make a significant difference in the percent products. In contrast, at 10 mM Fe(II) and pH 8.0, which is exactly on the ferrous hydroxide solubility line a noticeable difference in percent products is observed (**Figure 14**). For all ferrous hydroxide pH 8.0 reactors no degradation of TCE was detected (**Table 6, Figure 16**), but the presence of magnetite appeared to not only cause the reaction to occur, but also enhance the degradation of TCE by a factor of 5.

It is well reported through laboratory and field studies, that several reactive minerals have different reactivity towards various chlorinated solvents (He et al. 2015). But our results appear to show that a synergistic response between two minerals, magnetite with ferrous hydroxide, is occurring which lead to the degradation under conditions where ferrous hydroxide did not remove either PCE or TCE analytes alone (**Figures 14 & 16)**. Therefore, data for this study reports a strong case were reactivity of minerals towards chlorinated solvents can occur or enhance when different

mineral phases containing structural Fe(II) are investigated together, which we suggest is a closer representation of what occurs in nature or engineered systems.

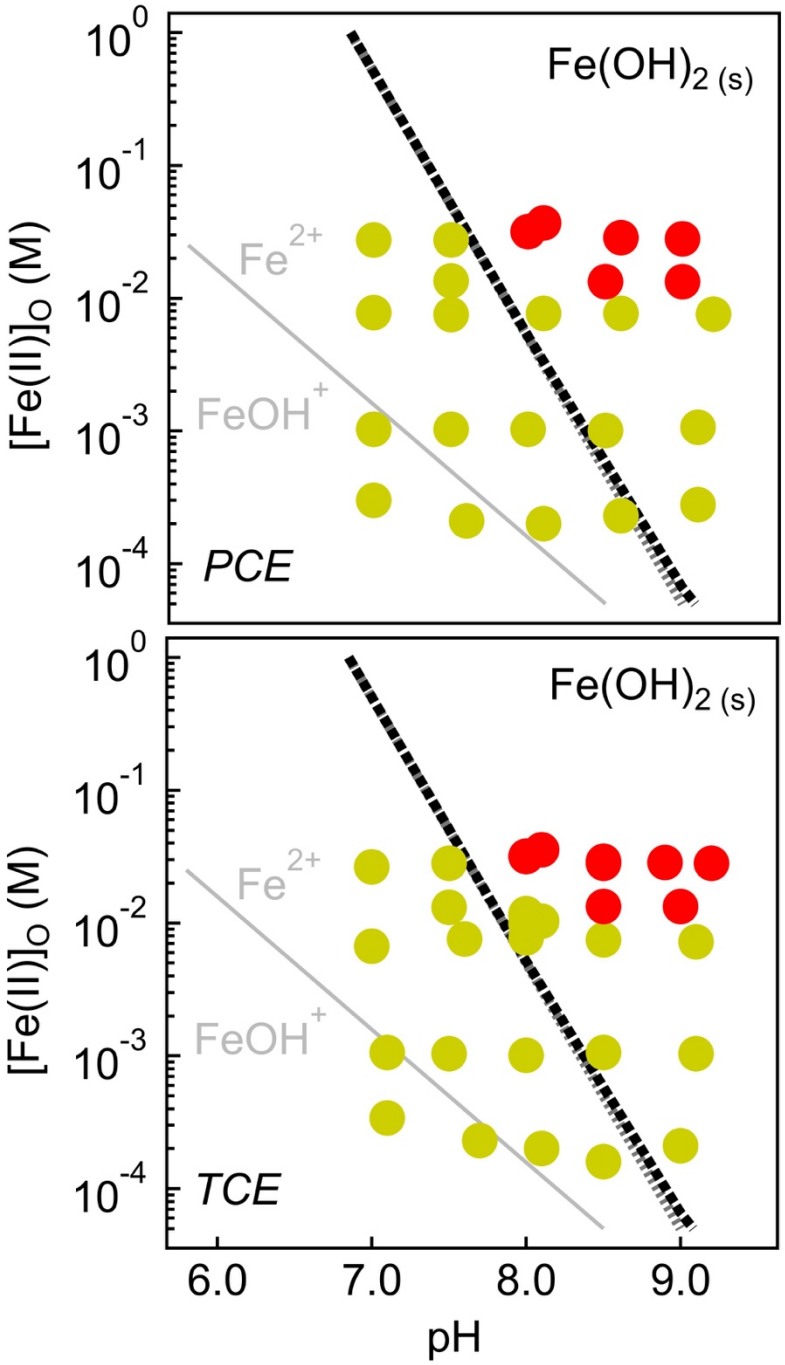

Figure 16. Fe(OH)2(s) solubility diagram with aqueous Fe(II) reactors without magnetite conditions overlaid, (a) PCE and (b) TCE. Red markers represent PCE and TCE reactors with reduction products (acetylene, ethylene and trace ethane). Ksp $[Fe(OH)_2(s)] = [Fe^{2+}] [OH^-]^2 = 5 \times 10^{-15}$ M (Sawyer, McCarty, and Parkin 2016).

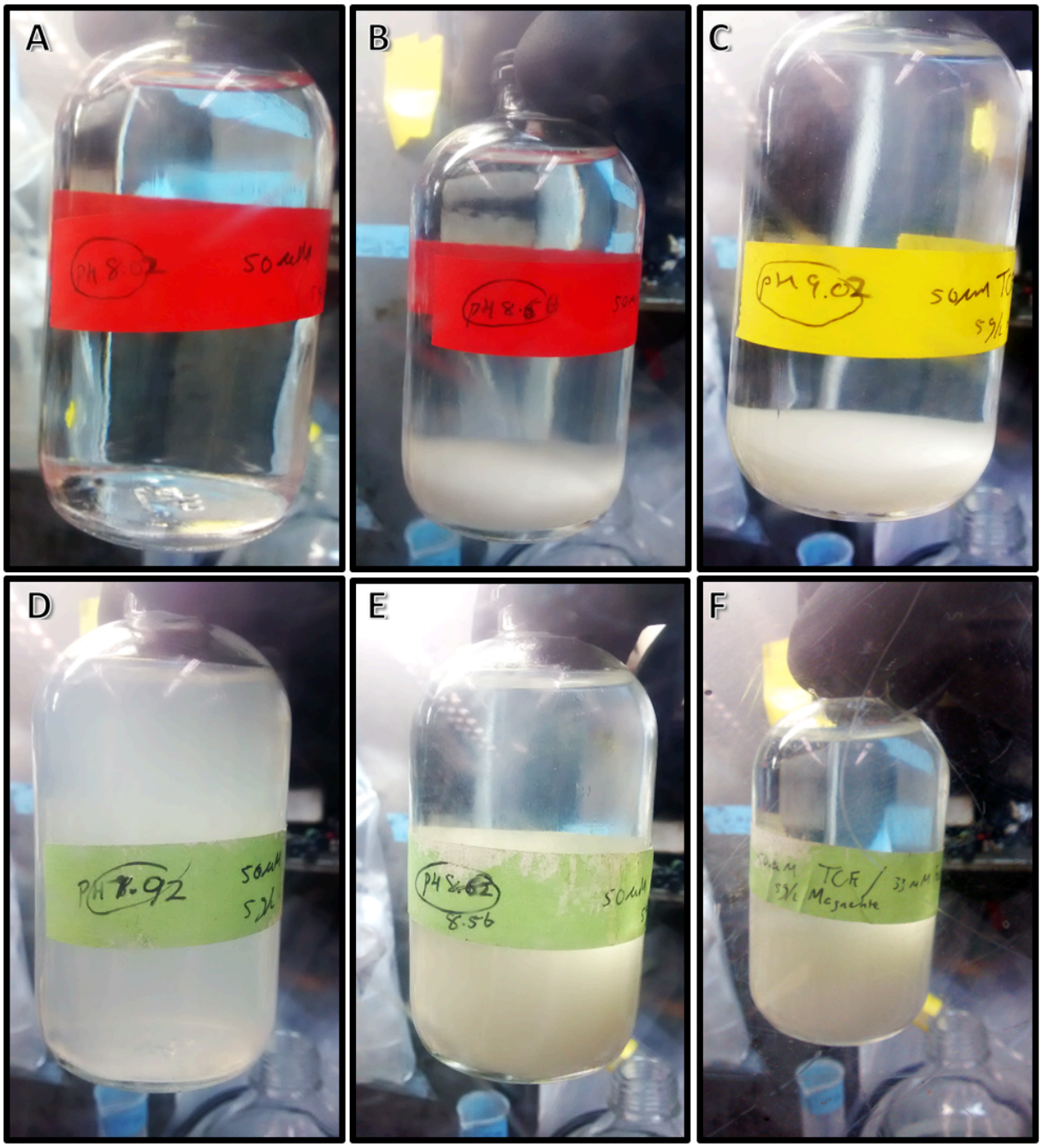

Figure 17. Reactors showing increasing saturation of white $Fe(OH)_2$ precipitate from left to right in buffer solution. A-C reactors are 7.0 mM initial Fe(II) concentration, set at pH values of 8.0, 8.5 and 9.0, respectively. D-F reactors are 30.0 mM initial Fe(II) concentration, set at pH values of 8.0, 8.5 and 9.0, respectively.

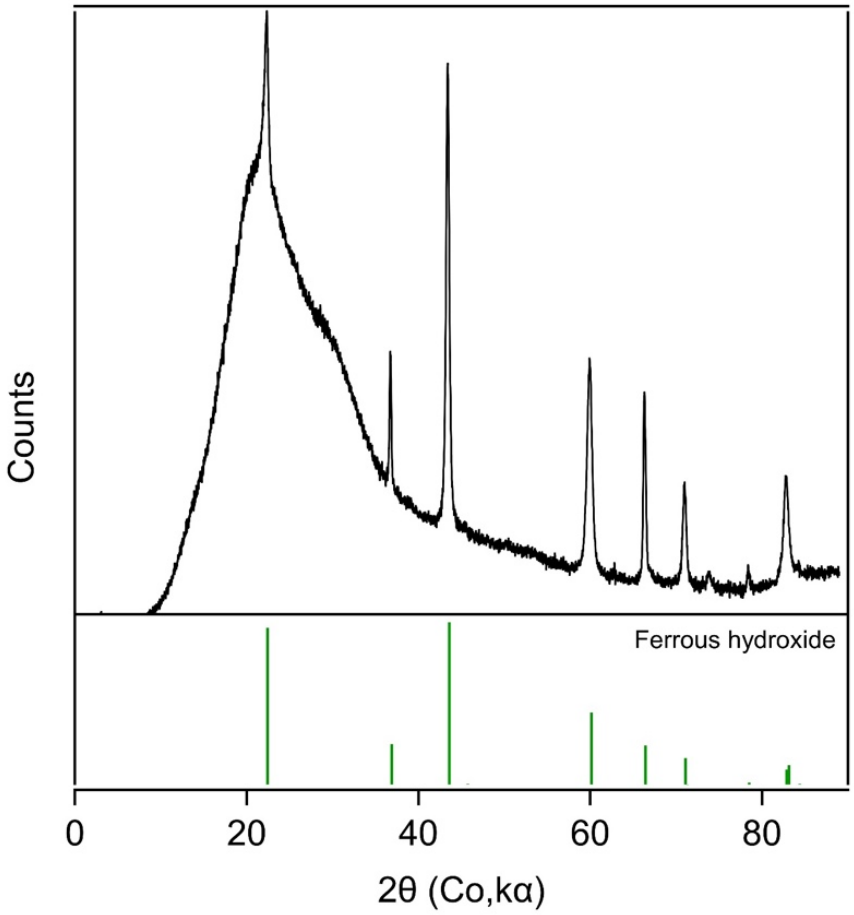

Figure 18. X-ray diffraction pattern of a TCE reactor with Fe(II) alone where 9.0% products were observed. Light green bars indicate ferrous hydroxide. Background between 12 and 34 is due to Kapton film used to seal the sample from being oxidized. Experimental conditions: 60 μM TCE, 10 mM MOPs/NaCl, 32 mM Fe(II), pH 8.

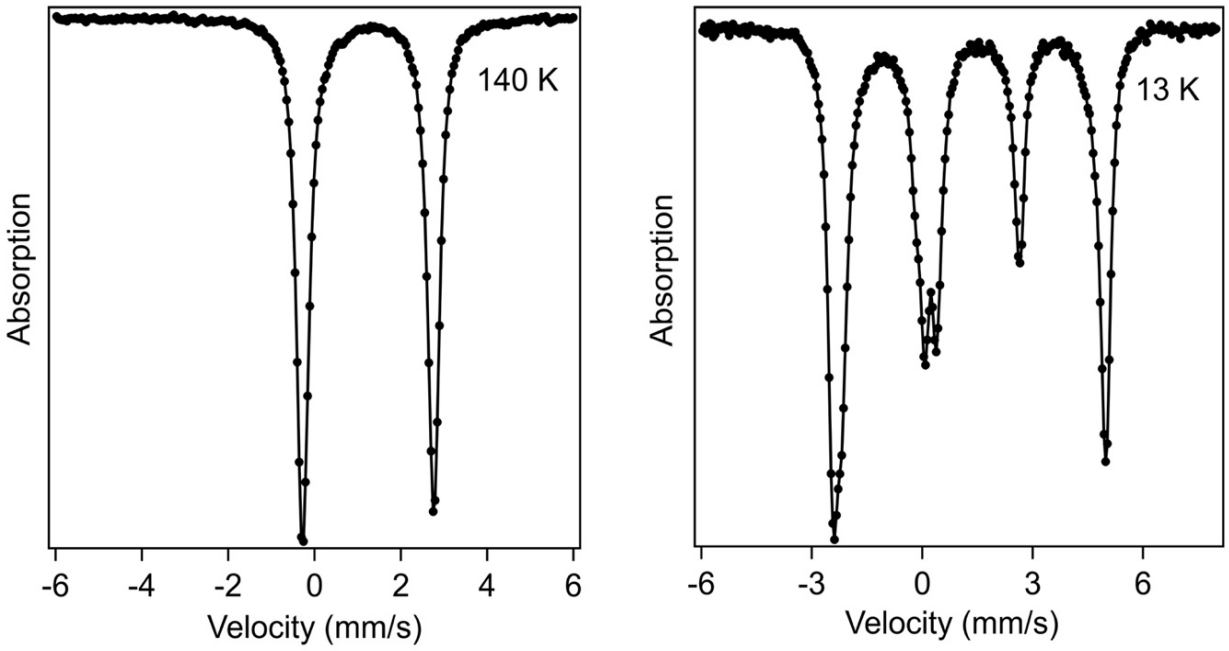

Figure 19. Mössbauer spectrum of white precipitate after reacting with 60 μM TCE, 10 mM MOPs/NaCl, pH 8.0, where 9.0% products were observed. Note: 32 mM Fe(II) was the initial concentration of dissolved iron added.

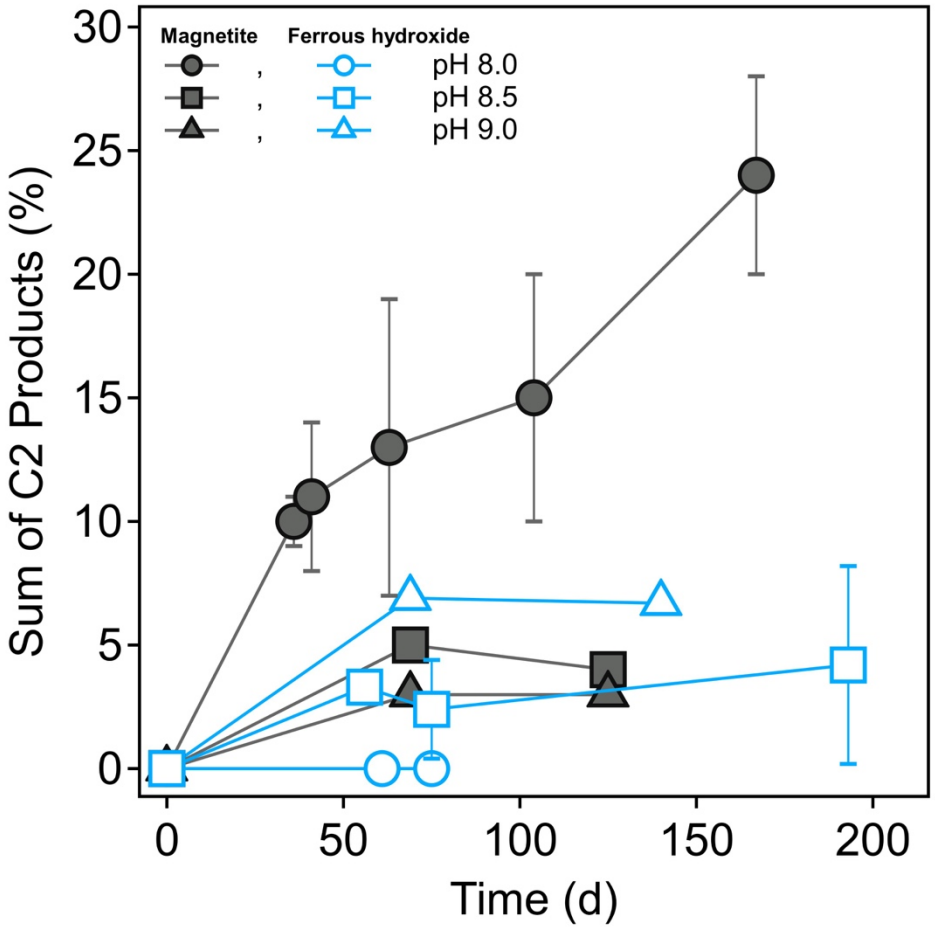

Figure 20. Sum of C2 products (acetylene, ethylene and ethane) formation for TCE reactors with ferrous hydroxide plus magnetite (Gray solid markers) and ferrous hydroxide alone (Blue open markers) over time. *Circles* are 10 mM Fe(II), pH 8.0. *Squares and triangles* are 30 mM Fe(II), pH 8.5-9.0.

Table 6. PCE/TCE with aqueous Fe(II) alone

Exp. #	$[C]_o$ µM	pH	$[Fe(II)]_o$ mM	IAP/K_{SP}	$[Fe(II)]_f$ mM	$[Fe(II)]_{loss}$ mM	% loss	% Products	% C recovery	Duration (days)
PCE										
67	58.2	7.0	0.30	0.001	0.16	-0.14	20	0	80	138
68	56.3	7.6	0.21	0.005	0.21	0	26.1	0	74	138
69	57.0	8.1	0.20	0.06	0.18	-0.02	21.9	0	78	138
70	59.1	8.6	0.23	0.60	0.20	-0.03	8.5	0	92	138
71	57.0	9.1	0.28	8.46	0.14	-0.14	19	0	81	138
72	55.2	7.0	1.03	0.002	1.08	0.05	29.6	0	82	134
73	56.1	7.5	1.03	0.023	1.06	0.03	20.4	0	70.4	134
74	57.2	8.0	1.03	0.24	1.04	0.01	16.4	0	80	134
75	53.6	8.5	1.01	2.23	1.02	0.01	16.4	0	84	134
76	52.7	9.1	1.07	28.16	0.37	-0.7	15.6	0	85	134
77	53.3	7.0	7.79	0.016	7.52	-0.27	19.1	0	81	117
78	51.2	7.5	7.52	0.165	7.17	-0.35	17.7	0	82	117
79	51.4	8.6	7.67	19.3	1.56	-6.11	15.9	0	84	117
80	55.7	9.2	7.58	317	1.15	-6.43	25.2	0	75	117
TCE										
81	51.9	7.1	0.34	0.001	0.33	-0.01	1.0	0	99	138
82	53.0	7.7	0.23	0.006	0.20	-0.03	2.4	0	98	138
83	52.5	8.1	0.20	0.065	0.24	0.04	11.1	0	89	138
84	53.8	8.5	0.16	0.37	0.25	0.09	4.5	0	96	138
85	52.1	9.0	0.21	3.51	0.16	-0.05	1.1	0	99	138
86	53.3	7.1	1.06	0.003	1.02	-0.04	4.1	0	96	134
87	53.5	7.5	1.04	0.023	1.08	0.04	4.1	0	96	134
88	51.7	8.0	1.01	0.194	1.06	0.05	2.2	0	98	134
89	52.7	8.5	1.03	2.26	1.00	-0.03	2.7	0	97	134
90	53.9	9.1	1.04	27.4	0.46	-0.58	6.3	0	94	134
91	49.4	7.0	6.71	0.013	8.08	1.37	1.0	0	99	117
92	51.1	7.6	7.59	0.20	7.64	0.05	1.0	0	99	117
93	53.5	8.0	7.71	1.62	6.27	-1.44	5.5	0	95	117
94	52.8	8.5	7.48	15.0	1.99	-5.49	6.5	0	94	117
95	52.0	9.1	7.23	209	0.88	-6.35	2.7	0	97	117

Note that reactors were set-up using 10 mM MOPs / NaCl or 10 mM PIPPs / NaCl buffers originally set at pH 7.00 and 8.5, respectively. MOPs buffer was used to set up all reactors within the pH range of (7.0 – 8.0), and the PIPPs for reactors (8.5- 9.0). All reactors were spiked with Fe(II) first, and tested for the reported **$[Fe(II)]_o$** mM values. Then the systems were pH adjusted using 2.5 or 10 M NaOH. A 500 µl sample was filtered removing precipitated solids and retested for **$[Fe(II)]_f$**. **$[Fe(II)]_{loss}$** is the difference of the final from the initial concentrations of determined ferrous iron. **% analtye loss, % Products** and **% Carbon recovery** are taken from the final reported time point. **Bolded** rows are used for reactors that a white cloudy precipitate was observed. The ion activity product (**IAP**) was determined with initial conditions for each experiment. **IAP/K_{sp}** values at equilibrium indicates the following w/ respects to potential Ferrous Hydroxide $Fe(OH)_2$ formation, **< 1 undersaturated, = 1 saturated, > 1 supersaturated** for a $K_{sp} = [Fe^{2+}] [OH^-]^2 = 5 * 10^{-15}$ mM and IAP determined from experimental **pH** and **$[Fe(II)]_o$** values.

Exp. #	$[C]_o$ µM	pH	$[Fe(II)]_o$ mM	IAP/K_{SP}	$[Fe(II)]_f$ mM	$[Fe(II)]_{loss}$ mM	% loss	% Products	% C recovery	Duration (days)	k_{obs} s^{-1}
PCE											
96	50.2	8.0	31.7	6.34	1.99	-29.7	27.6	2.7	75	193	1.9×10^{-8}
97	54.0	8.6	28.52	75.20	1.39	-27.13	39.0	0.3	61	188	3.0×10^{-8}
98	44.4	9.0	28.00	465.83	0.63	-27.37	11.9	2.0	90	188	7.7×10^{-9}
99	54.0	8.1	36.80	12.79	33.99	-2.81	23.3	1.1	77	156	2.1×10^{-8}
100	50.2	7.0	27.41	0.05	n.d.	n.d.	16	0	84	140	0
101	50.3	7.5	27.32	0.52	n.d.	n.d.	14	0	78	140	0
102	49.2	7.5	13.52	0.30	n.d.	n.d.	13	0	87	140	0
103	52.7	8.5	~13.34	26.68	n.d.	n.d.	14	1.0	86	140	1.3×10^{-8}
104	51.2	9.0	~13.34	266.8	n.d.	n.d.	19	1.0	74	140	1.8×10^{-8}
TCE											
105	~50	8.0	11.79	2.36	n.d.	n.d.	6.3	0	94	75	0
106	~50	8.0	11.54	2.31	n.d.	n.d.	3.1	0	97	75	0
107	~50	8.0	10.27	2.05	n.d.	n.d.	2.3	0	98	75	0
108	79.9	8.0	11.64	2.33	n.d.	n.d.	35	0	65	75	0
109	152.9	8.0	9.90	1.98	n.d.	n.d.	-36.6	0	33.2	75	0
110	66.3	8.0	9.84	1.97	n.d.	n.d.	23.5	0	77	75	0
111	58.9	8.0	31.98	6.40	15.19	-16.79	26.6	9.0	82	193	4.7×10^{-8}
112	196.9	8.0	31.62	6.32	9.39	-22.23	-21.5	3.8	125	193	-
113	52.6	8.1	35.66	8.98	33.90	-1.76	7.0	8.0	100.6	156	5.5×10^{-9}
114	50.9	8.5	29.21	64.1	1.57	-27.64	-7.9	1.2	109	193	-
115	50.2	8.5	28.26	64.9	1.73	-26.53	5.0	7.2	102	193	2.9×10^{-9}
116	51.0	8.9	28.55	433	0.46	-28.09	7.4	9.0	102	193	4.6×10^{-9}
117	51.5	9.2	28.08	1173	0.33	-27.75	23.3	13.0	90	193	1.6×10^{-8}
118	54.1	7.0	26.54	0.05	n.d.	n.d.	21	0	79	140	0
119	56.9	7.5	28.16	0.56	n.d.	n.d.	16	0	84	140	0
120	52.6	7.5	13.13	0.26	n.d.	n.d.	14	0	86	140	0
121	56.2	8.5	~13.34	26.68	n.d.	n.d.	29	6	75	140	2.8×10^{-8}
122	55.6	9.0	~13.34	266.8	n.d.	n.d.	24	7	83	140	2.3×10^{-8}

Note that reactors were set-up using 10 mM MOPs / NaCl or 10 mM PIPPs / NaCl buffers originally set at pH 7.00 and 8.5, respectively. MOPs buffer was used to set up all reactors within the pH range of (7.0 – 8.0), and the PIPPs for reactors (8.5- 9.0). All reactors were spiked with Fe(II) first, and tested for the reported **$[Fe(II)]_o$** mM values. Then the systems were pH adjusted using 2.5 or 10 M NaOH. A 500 µl sample was filtered removing precipitated solids and retested for **$[Fe(II)]_f$**. **$[Fe(II)]_{loss}$** is the difference of the final from the initial concentrations of determined ferrous iron. **% analtye loss, % Products** and **% Carbon recovery** are taken from the final reported time point. **Bolded** rows are used for reactors that a white cloudy precipitate was observed. The ion activity product (**IAP**) was determined with initial conditions for each experiment. **IAP/K_{sp}** values at equilibrium indicates the following w/ respects to potential Ferrous Hydroxide $Fe(OH)_2$ formation, **< 1 undersaturated, = 1 saturated, > 1 supersaturated** for a $K_{sp} = [Fe^{2+}] [OH^-]^2 = 5 * 10^{-15}$ mM and IAP determined from experimental **pH** and **$[Fe(II)]_o$** values.

CHAPTER III

ENGINEERING SIGNIFICANCE AND CONCLUSION

Human development has resulted in the release of tons of anthropogenic compounds like tetrachloroethylene (PCE) and trichloroethylene (TCE) at unlined landfills, leaking underground storage tanks, and soils that threaten our ecosystem and the future state of hundreds of groundwater resources (Kueper et al. 2014; Meckenstock et al. 2015; Tratnyek et al. 2014). Groundwater is a crucial water source for many countries worldwide (Zektser, Loáiciga, and Wolf 2005). The United States is not exempt, where it is estimated that one-half of the nation's population depend on groundwater as a drinking-water source for residents in rural areas (Zogorski et al. 2006). Finding sustainable engineered solutions to contain, and or remediate plumes of PCE and TCE is of top priority to avoid further contamination within the groundwater table from dissolve phase organics reaching existing drinking water wells. Feasible solutions must address the current economic burden and environmental impacts due primarily from decades of reliance on energy intensive and carbon dioxide (CO_2) emitting approaches, like pump and treat (Vörösmarty et al. 2000; Kueper et al. 2014; He et al. 2009). Moreover, an effective strategy must degrade the parent chlorinated solvents to less benign products (i.e., Acetylene) and not stall at other carcinogenic volatile organic compounds VOCs, such as dichloroethenes or vinyl chloride (He et al. 2009).

Reductive elimination of PCE and TCE is suggested as the major abiotic degradation pathway when reacted with iron Fe(II)-bearing minerals (Cwiertny and Scherer 2010; He et al. 2015). The most common transformation product from reductive elimination with Fe(II) containing minerals is acetylene, which is suggested as a signature abiotic product (He et al. 2015).

For this study, all PCE and TCE reactions had acetylene as the major transformation product, confirming another situation where reductive elimination is the dominant degradation pathway, similar to other Fe(II) containing minerals such as mackinawite FeS, Green rust, and Fe^{2+}-sorbed minerals (He et al. 2015).

It is important to be able to predict pathways for abiotic degradation, and estimate the rates at which a specific reactive iron minerals may degrade targeted chlorinated solvents. We know reactive Fe(II)-containing minerals such as magnetite and green rust form under iron reducing conditions within engineered remedies i.e., zero valent iron permeable reactive barriers (PRBs), enhanced reductive dechlorination (ERD) treatment zones, and naturally in aquifers (He et al. 2015; Vodyanitskii 2014). Therefore, it is worth continued effort exploring magnetite as a potential mineral phase that can be incorporated as part of existing remedies. Before this study, the optimal geochemical conditions for magnetite driven degradation of PCE and TCE under iron reducing conditions were not fully explored (**Table 1**). In the literature, much greater effort has been spent to determine whether other reactive minerals such as mackinawite, green rust and pyrite degrade PCE and TCE, and whether they can be effectively incorporated into engineered remediation strategies under reducing groundwater conditions (He et al. 2015).

An advancing engineered treatment strategy for chlorinated ethenes is monitored natural attenuation (MNA), where the site specific reactive biogeochemical makeup is utilized to decrease the concentration of contaminants (Kueper et al. 2014). Reactive Fe(II)-bearing minerals for abiotic degradation of chlorinated solvents in aquifers is an important contributor to natural attenuation. Although magnetite Fe_3O_4 is often present in unconsolidated glacial aquifers and aquifers that form in sediments that are shed by uplands composed of granite or other igneous

rocks (Darlington and Rectanus 2015), our results highlight that simply monitoring for the presence of magnetite alone does not readily tell whether PCE and TCE will degrade.

For this study, it was discovered that magnetite under iron reducing conditions where ferrous hydroxide $Fe(OH)_2$ is likely to precipitate, degradation of PCE and TCE occurs. Therefore, groundwater engineers performing site characterization, assessment and even modelling of natural attenuation for PCE and TCE should keenly evaluate changes to aqueous Fe(II) concentrations, and the quantity of magnetite within contaminated aquifers (Thornton, Lerner, and Banwart 2001). Particularly, for groundwater plumes with low dissolved concentrations of the target organic contaminants.

Though our findings indicate that the solid-state chemistry of magnetite i.e., stoichiometry does not directly enhance the rate of degradation for both PCE and TCE as originally hypothesized, our results confirm that exclusively at conditions where magnetite is expected to be stoichiometric $x = 0.5$ in the presence of precipitated $Fe(OH)_2$, degradation of the target chlorinated ethenes occurred. This finding strongly supports the notion that the mineral stoichiometry of magnetite should always be evaluated as an intrinsic identifier for the select batch of mineral used within laboratory experiments, especially to ensure experimental reproducibility and evaluating redox processes of contaminants with magnetite (Gorski and Scherer 2009b; Latta et al. 2011; Wylie, Olive, and Powell 2016).

To evaluate the quantity of magnetite mineral present in aquifer sediments, magnetic susceptibility of magnetite from downhole sondes (probes) is a promising technique (Wiedemeier et al. 2017; Ferrey et al. 2004b). To our understanding a similar quantification technique to determine the quantity of meta-stable mineral states like green rust, or ferrous hydroxide at field

scale is not readily available, but it appears that some work was done to report a signature magnetic susceptibility values for pure and partially oxidized ferrous hydroxide (Zernike 1953).

For this study, in situ precipitation of ferrous hydroxide was evaluated under such a wide range of conditions in the presence of magnetite, our data set seems to indicate that the optimal geochemical conditions for TCE dechlorination was demonstrated as directly at the $Fe(OH)_2$ solubility curve (pH 8 and 10 mM Fe(II) with 5 g/l Magnetite) (**Figure 20**). The apparent difference between PCE and TCE degradation by ferrous hydroxide alone, and the synergistic response with magnetite plus ferrous hydroxide, is quite an interesting finding and presents some potential future research questions.

1. Does $Fe(OH)_2$ (s) in the presence of magnetite enhance the rate of degradation of dicholroethenes DCEs, since DCEs were not detected in any of our PCE and TCE reactors?

Rationale:

   a. At the field-scale, microcosm studies was used to show the first case of non-biological degradation evidence for DCEs from sediment that contain magnetite (Ferrey et al. 2004b).

   b. From laboratory studies, it was suggested that in situ formed magnetite with other mineral phases present does not react with cis-DCE, but Ferrous hydroxide and green rust formed in situ did (Jeong et al. 2011; Jeong et al. 2013).

2. Why did our results appear to indicate that when ferrous hydroxide alone reacted with PCE and TCE needed a significant build up/ mass loading of the solids or electrons to be present for degradation to occur?

3. Does a synergistic response, as observed for magnetite plus ferrous hydroxide PCE and TCE degradation occur with other reactive minerals like ferrous hydroxide plus troilite, pyrite or mackinawite?

For groundwater remediation, abiotic reactions are being engineered to stimulate reactive mineral formation, as in the case of biogeochemical reductive dechlorination (BiRD) technology

(He et al. 2015; Kennedy et al. 2006; Kennedy, Everett, and Gonzales 2006). The BiRD method simulates bio-reactivity of sulfate-reducing bacteria, through amending a groundwater site with sulfate SO_4^{2-} and if needed a source of organic carbon is introduced to the sediments containing mineral irons like magnetite. Due to successful field testing of this technology, it is worth performing similar controlled kinetic laboratory experiments to investigate the degradation rates, and transformation products for chlorinated ethenes PCE and TCE by magnetite under sulfur-reducing conditions.

APPENDIX

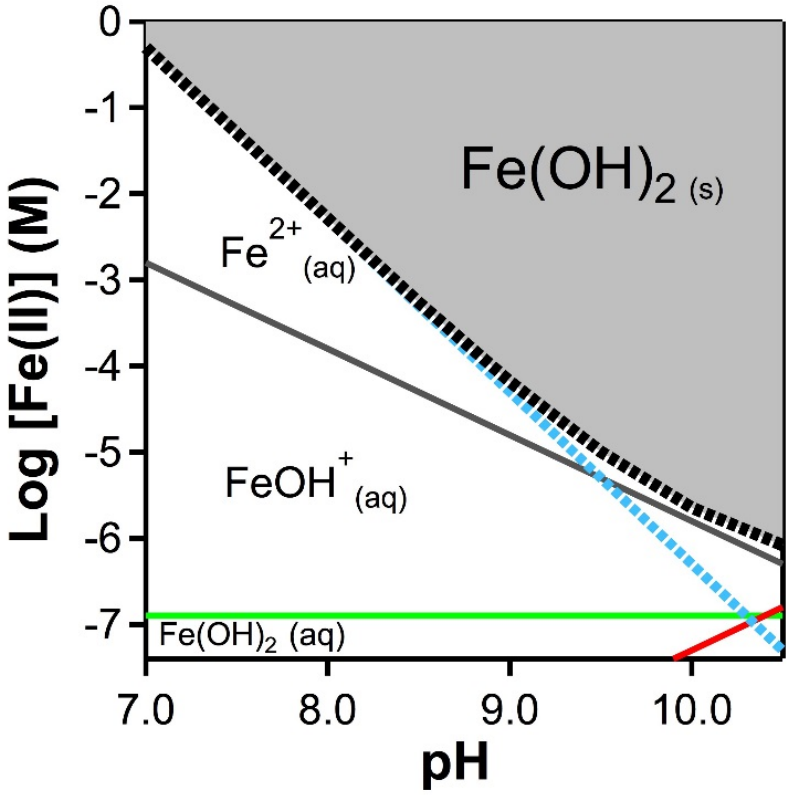

Figure 21. Sample ferrous hydroxide ($Fe(OH)_2$) solubility diagram.

Equations:

Line 1

$log[Fe^{2+}] = 13.7 - 2\,pH$

Line 2

$log[FeOH^{+}] = 4.2 - pH$

Line 3

$log\left[Fe(OH)_{2\,aq}\right] = -6.9$

Line 4

$log[Fe(OH)_3^-] = -17.3 + pH$

Solubility Curve:

$$S_T = [Fe^{2+}] + [FeOH^{+}] + \left[Fe(OH)_{2\,aq}\right] + [Fe(OH)_3^-]$$

Sample of Henry's Law Calculations

For a Carbon Mass Balance

Mass balance equation - MBE **(Closed system)**
Input + generation – output – consumption = accumulation

Carbon atomic balance **(2 phase system)**

Total Carbon$_{PCE\ (aq)}$ = C$_{PCE\ (aq\ \&\ g)}$ + C$_{TCE\ (aq\ \&\ g)}$ + C$_{Ethane\ (aq\ \&\ g)}$ + C$_{ethylene\ (aq\ \&\ g)}$ + C$_{acetylene\ (aq\ \&\ g)}$

Determination of specie specific dimensionless Henry's coefficient H^{cc}

$$H^{cc}_{PCE} = 6.2 \times 10^{-4}\ \frac{mol}{m^3\ Pa} \times 8.314\ \frac{m^3\ Pa}{mol\ K} \times 298\ K = 1.54$$

$$H^{cc}_{TCE} = 1.02 \times 10^{-3}\ \frac{mol}{m^3\ Pa} \times 8.314\ \frac{m^3\ Pa}{mol\ K} \times 298\ K = 2.55$$

$$H^{cc}_{Ethane} = 1.9 \times 10^{-5}\ \frac{mol}{m^3\ Pa} \times 8.314\ \frac{m^3\ Pa}{mol\ K} \times 298\ K = 0.047$$

$$H^{cc}_{Ethylene} = 1.9 \times 10^{-5}\ \frac{mol}{m^3\ Pa} \times 8.314\ \frac{m^3\ Pa}{mol\ K} \times 298\ K = 0.047$$

$$H^{cc}_{Acetylene} = \_\_\_\_\_\ \frac{mol}{m^3\ Pa} \times 8.314\ \frac{m^3\ Pa}{mol\ K} \times 298\ K = n.d.$$

Henry's Law

$H^{cc}_{PCE/TCE} = H^{cp} * RT$

- H^{cc} – dimensionless
- H^{cp} – (mol/m^{3}Pa)
- R – 8.314 (m^3 Pa/ mol K)

$H^{cc}_{PCE/TCE} = C_{aq}/C_g$

$$\textbf{Percent Recovery} = \frac{(Analytically\ determined\ \ carbon + Henry's\ Law\ determined\ carbon)}{Spiked\ total\ carbon} \times 100$$

Determination of gas/liquid phase concentrations using H^{cc}

$$C_{gPCE} = Ca_{PCE}/H^{CC}_{PCE} =$$

$$C_{gTCE} = Ca_{TCE}/H^{CC}_{TCE} =$$

$$C_{aqEthane} = H^{CC}_{Ethane} * Cg_{Ethane} =$$

$$C_{aqEthylene} = H^{CC}_{Ethylene} * Cg_{Ethylene} =$$

$$C_{aqAcetylene} = H^{CC}_{Acetylene} * Cg_{Acetylene} =$$

Carbon atomic mass balance (2 phase system)

Input Carbon atoms = Output Carbon Atom

$$Total\ C_{PCE\ (aq)} = \sum C_{PCE\ (aq\ \&\ g)} + \sum C_{TCE\ (aq\ \&\ g)} + \sum C_{Ethane\ (aq\ \&\ g)} + \sum C_{Ethylene\ (aq\ \&\ g)} + \sum C_{Acetylene\ (aq\ \&\ g)}$$

Converted concentration to moles of carbon.

REFERENCES

1. Arnold, William A, and A Lynn Roberts. 2000. 'Pathways and kinetics of chlorinated ethylene and chlorinated acetylene reaction with Fe (0) particles', *Environmental Science & Technology*, 34: 1794-805.

2. Barnes, Kimberlee K, Dana W Kolpin, Edward T Furlong, Steven D Zaugg, Michael T Meyer, and Larry B Barber. 2008. 'A national reconnaissance of pharmaceuticals and other organic wastewater contaminants in the United States—I) Groundwater', *Science of the total environment*, 402: 192-200.

3. Bazylinski, D. A., R. B. Frankel, B. R. Heywood, S. Mann, J. W. King, P. L. Donaghay, and A. K. Hanson. 1995. 'Controlled Biomineralization of Magnetite (Fe3o4) and Greigite (Fe3s4) in a Magnetotactic Bacterium', *Applied and Environmental Microbiology*, 61: 3232-39.

4. Bazylinski, D. A., R. B. Frankel, and K. O. Konhauser. 2007. 'Modes of biomineralization of magnetite by microbes', *Geomicrobiology Journal*, 24: 465-75.

5. Borch, Thomas, Ruben Kretzschmar, Andreas Kappler, Philippe Van Cappellen, Matthew Ginder-Vogel, Andreas Voegelin, and Kate Campbell. 2009. 'Biogeochemical redox processes and their impact on contaminant dynamics', *Environmental Science & Technology*, 44: 15-23.

6. Bradley, Paul M, and Francis H Chapelle. 1997. 'Kinetics of DCE and VC mineralization under methanogenic and Fe (III)-reducing conditions', *Environmental Science & Technology*, 31: 2692-96.

7. Cassman, Kenneth G, Achim Dobermann, and Daniel T Walters. 2002. 'Agroecosystems, nitrogen-use efficiency, and nitrogen management', *AMBIO: A Journal of the Human Environment*, 31: 132-40.

8. Chang, S. B. R., J. F. Stolz, J. L. Kirschvink, and S. M. Awramik. 1989. 'Biogenic Magnetite in Stromatolites .2. Occurrence in Ancient Sedimentary Environments', *Precambrian Research*, 43: 305-15.

9. Chiu, Weihsueh A, Jennifer Jinot, Cheryl Siegel Scott, Susan L Makris, Glinda S Cooper, Rebecca C Dzubow, Ambuja S Bale, Marina V Evans, Kathryn Z Guyton, and Nagalakshmi Keshava. 2013. 'Human health effects of trichloroethylene: key findings and scientific issues', *Environmental Health Perspectives (Online)*, 121: 303.

10. Cundy, Andrew B, Laurence Hopkinson, and Raymond LD Whitby. 2008. 'Use of iron-based technologies in contaminated land and groundwater remediation: a review', *Science of the total environment*, 400: 42-51.

11. Cwiertny, David M, and Michelle M Scherer. 2010. 'Chlorinated solvent chemistry: Structures, nomenclature and properties.' in, *In Situ Remediation of Chlorinated Solvent Plumes* (Springer).

12. Doherty, Richard E. 2000a. 'A history of the production and use of carbon tetrachloride, tetrachloroethylene, trichloroethylene and 1, 1, 1-trichloroethane in the United States: Part 1--historical background; carbon tetrachloride and tetrachloroethylene', *Environmental forensics*, 1: 69-81.

13. ———. 2000b. 'A History of the Production and Use of Carbon Tetrachloride, Tetrachloroethylene, Trichloroethylene and 1, 1, 1-Trichloroethane in the United States: Part 2—Trichloroethylene and 1, 1, 1-Trichloroethane', *Environmental forensics*, 1: 83-93.

14. Ferrey, M. L., R. T. Wilkin, R. G. Ford, and J. T. Wilson. 2004a. 'Nonbiological removal of cis-dichloroethylene and 1,1-dichloroethylene in aquifer sediment containing magnetite', *Environmental Science & Technology*, 38: 1746-52.

15. Ferrey, Mark L, Richard T Wilkin, Robert G Ford, and John T Wilson. 2004b. 'Nonbiological removal of cis-dichloroethylene and 1, 1-dichloroethylene in aquifer sediment containing magnetite', *Environmental Science & Technology*, 38: 1746-52.

16. Genin, J. M., Ph. Bauer, A. A. Olowe, and D. Rezel. 1986. 'Mössbauer study of the kinetics of simulated corrosion process of iron in chlorinated aqueous solution around room temperature: The hyperfine structure of ferrous hydroxides and Green Rust I', *Hyperfine Interactions*, 29: 1355-60.

17. Gorski, C. A., J. T. Nurmi, P. G. Tratnyek, T. B. Hofstetter, and M. M. Scherer. 2010. 'Redox Behavior of Magnetite: Implications for Contaminant Reduction', *Environmental Science & Technology*, 44: 55-60.

18. Gorski, C. A., and M. M. Scherer. 2009a. 'Influence of Magnetite Stoichiometry on Fe-II Uptake and Nitrobenzene Reduction', *Environmental Science & Technology*, 43: 3675-80.

19. ———. 2010a. 'Determination of nanoparticulate magnetite stoichiometry by Mossbauer spectroscopy, acidic dissolution, and powder X-ray diffraction: A critical review', *American Mineralogist*, 95: 1017-26.

20. ———. 2011a. 'Fe2+ Sorption at the Fe Oxide-Water Interface: A Revised Conceptual Framework', *Aquatic Redox Chemistry*, 1071: 315-43.

21. Gorski, Christopher A, and Matthew S Fantle. 2017. 'Stable mineral recrystallization in low temperature aqueous systems: A critical review', *Geochimica et Cosmochimica Acta*, 198: 439-65.

22. Gorski, Christopher A, James T Nurmi, Paul G Tratnyek, Thomas B Hofstetter, and Michelle M Scherer. 2009. 'Redox behavior of magnetite: Implications for contaminant reduction', *Environmental Science & Technology*, 44: 55-60.
23. Gorski, Christopher A, and Michelle M Scherer. 2009b. 'Influence of magnetite stoichiometry on FeII uptake and nitrobenzene reduction', *Environmental Science & Technology*, 43: 3675-80.

24. ———. 2010b. 'Determination of nanoparticulate magnetite stoichiometry by Mössbauer spectroscopy, acidic dissolution, and powder X-ray diffraction: A critical review', *American Mineralogist*, 95: 1017-26.

25. ———. 2011b. 'Fe2+ sorption at the Fe oxide-water interface: A revised conceptual framework', *Aquatic Redox Chemistry*, 1071: 477-517.

26. Gupta, Shreekant, George Van Houtven, and Maureen Cropper. 1996. 'Paying for permanence: an economic analysis of EPA's cleanup decisions at Superfund sites', *The RAND Journal of Economics*: 563-82.

27. Guyton, Kathryn Z, Karen A Hogan, Cheryl Siegel Scott, Glinda S Cooper, Ambuja S Bale, Leonid Kopylev, Stanley Barone Jr, Susan L Makris, Barbara Glenn, and Ravi P Subramaniam. 2014. 'Human health effects of tetrachloroethylene: key findings and scientific issues', *Environmental Health Perspectives (Online)*, 122: 325.

28. Hansel, Colleen M, Shawn G Benner, and Scott Fendorf. 2005. 'Competing Fe (II)-induced mineralization pathways of ferrihydrite', *Environmental Science & Technology*, 39: 7147-53.

29. Hansel, Colleen M, Shawn G Benner, Jim Neiss, Alice Dohnalkova, Ravi K Kukkadapu, and Scott Fendorf. 2003. 'Secondary mineralization pathways induced by dissimilatory iron reduction of ferrihydrite under advective flow', *Geochimica et Cosmochimica Acta*, 67: 2977-92.

30. Hawley, E. L., R. A. Deeb, and H. Levine. 2014. 'Groundwater Remediation and the Use of Alternative Endpoints at Highly Complex Sites', *Chlorinated Solvent Source Zone Remediation*, 7: 627-52.

31. He, Y, C Su, J Wilson, R Wilkin, C Adair, T Lee, P Bradley, and M Ferrey. 2009. 'Identification and characterization methods for reactive minerals responsible for natural attenuation of chlorinated organic compounds in ground water', *US EPA*.

32. He, Y Thomas, John T Wilson, and Richard T Wilkin. 2010. 'Impact of iron sulfide transformation on trichloroethylene degradation', *Geochimica et Cosmochimica Acta*, 74: 2025-39.

33. He, YT, JT Wilson, C Su, and RT Wilkin. 2015. 'Review of abiotic degradation of chlorinated solvents by reactive iron minerals in aquifers', *Groundwater Monitoring & Remediation*, 35: 57-75.

34. Hyun, Sung Pil, and Kim F Hayes. 2015. 'Abiotic reductive dechlorination of cis-DCE by ferrous monosulfide mackinawite', *Environmental Science and Pollution Research*, 22: 16463-74.

35. Jeong, Hoon Y, Karthik Anantharaman, Young-Soo Han, and Kim F Hayes. 2011. 'Abiotic reductive dechlorination of cis-dichloroethylene by Fe species formed during iron-or sulfate-reduction', *Environmental Science & Technology*, 45: 5186-94.

36. Jeong, Hoon Y, Karthik Anantharaman, Sung P Hyun, Moon Son, and Kim F Hayes. 2013. 'pH impact on reductive dechlorination of cis-dichloroethylene by Fe precipitates: An X-ray absorption spectroscopy study', *Water research*, 47: 6639-49.

37. Kavanaugh, M, R Deeb, and E Hawley. 2011. "Diagnostic tools for performance evaluation of innovative in-situ remediation technologies at chlorinated solvent-contaminated sites, Final Report for ESTCP Project ER-200318; Environmental Security Technology Certification Program." In.

38. Kennedy, Lonnie G, Jess W Everett, Erica Becvar, and Donald DeFeo. 2006. 'Field-scale demonstration of induced biogeochemical reductive dechlorination at Dover Air Force Base, Dover, Delaware', *Journal of contaminant hydrology*, 88: 119-36.

39. Kennedy, Lonnie G, Jess W Everett, and James Gonzales. 2006. 'Assessment of biogeochemical natural attenuation and treatment of chlorinated solvents, Altus Air Force Base, Altus, Oklahoma', *Journal of contaminant hydrology*, 83: 221-36.

40. Kueper, Bernard H, Hans F Stroo, Catherine M Vogel, and C Herb Ward. 2014. *Chlorinated solvent source zone remediation* (Springer).

41. Latta, D. E., C. A. Gorski, M. I. Boyanov, E. J. O'Loughlin, K. M. Kemner, and M. M. Scherer. 2012. 'Influence of Magnetite Stoichiometry on U-VI Reduction', *Environmental Science & Technology*, 46: 778-86.

42. Latta, Drew E, Christopher A Gorski, Maxim I Boyanov, Edward J O'Loughlin, Kenneth M Kemner, and Michelle M Scherer. 2011. 'Influence of magnetite stoichiometry on UVI reduction', *Environmental Science & Technology*, 46: 778-86.

43. Lee, MD, JM Odom, and RJ Buchanan Jr. 1998. 'New perspectives on microbial dehalogenation of chlorinated solvents: insights from the field', *Annual Reviews in Microbiology*, 52: 423-52.

44. Lee, W., and B. Batchelor. 2002a. 'Abiotic reductive dechlorination of chlorinated ethylenes by iron-bearing soil minerals. 1. Pyrite and magnetite', *Environmental Science & Technology*, 36: 5147-54.

45. Lee, Woojin, and Bill Batchelor. 2002b. 'Abiotic reductive dechlorination of chlorinated ethylenes by iron-bearing soil minerals. 1. Pyrite and magnetite', *ENVIRONMENTAL SCIENCE AND TECHNOLOGY-WASHINGTON DC-*, 36: 5147-54.

46. Liang, Xiaoming, R Paul Philp, and Elizabeth C Butler. 2009a. 'Kinetic and isotope analyses of tetrachloroethylene and trichloroethylene degradation by model Fe (II)-bearing minerals', *Chemosphere*, 75: 63-69.

47. Liang, Xiaoming, R. Paul Philp, and Elizabeth C. Butler. 2009b. 'Kinetic and isotope analyses of tetrachloroethylene and trichloroethylene degradation by model Fe(II)-bearing minerals', *Chemosphere*, 75: 63-69.

48. Lovley, D. R., J. F. Stolz, G. L. Nord, and E. J. P. Phillips. 1987. 'Anaerobic Production of Magnetite by a Dissimilatory Iron-Reducing Microorganism', *Nature*, 330: 252-54.

49. Madigan, Michael T, David P Clark, David Stahl, and John M Martinko. 2010. *Brock Biology of Microorganisms 13th edition* (Benjamin Cummings).

50. McCarty, Perry L, HF Stroo, and CH Ward. 2010. 'In situ remediation of chlorinated solvent plumes'.

51. Meckenstock, Rainer U, Martin Elsner, Christian Griebler, Tillmann Lueders, Christine Stumpp, Jens Aamand, Spiros N Agathos, Hans-Jørgen Albrechtsen, Leen Bastiaens, and Poul L Bjerg. 2015. "Biodegradation: updating the concepts of control for microbial cleanup in contaminated aquifers." In.: ACS Publications.

52. Miyamoto, H., T. Shinjo, and T. Takada. 1967. 'Mossbauer effect of the ^{57}Fe in $Fe(OH)_2$', *Journal of the physical society of Japan*, 23: 1421.

53. Nealson, K. H., and C. R. Myers. 1992. 'Microbial Reduction of Manganese and Iron - New Approaches to Carbon Cycling', *Applied and Environmental Microbiology*, 58: 439-43.

54. Pankow, James F, and John A Cherry. 1996. 'Dense chlorinated solvents and other DNAPLs in groundwater: History, behavior, and remediation'.

55. Pennisi, E. 2002. 'Geobiologists: As diverse as the bugs they study', *Science*, 296: 1058-60.

56. Sander, R. 2015. 'Compilation of Henry's law constants (version 4.0) for water as solvent', *Atmospheric Chemistry and Physics*, 15: 4399-981.

57. Sawyer, Clair N, Perry L McCarty, and Gene F Parkin. 2016. 'Chemistry for environmental engineering and science'.

58. Sivavec, Timothy Mark. 1998. "Composition and method for ground water remediation." In.: Google Patents.

59. Squillace, Paul J, Michael J Moran, Wayne W Lapham, Curtis V Price, Rick M Clawges, and John S Zogorski. 1999. 'Volatile organic compounds in untreated ambient groundwater of the United States, 1985-1995', *Environmental Science & Technology*, 33: 4176-87.

60. Stroo, Hans F, John T Wilson, Patrick J Evans, Carmen A Lebron, Bruce M Henry, Drew E Latta, Rajat S Ghosh, and Andrea Leeson. 2015. "In Situ Biogeochemical Treatment Demonstration: Lessons Learned from ESTCP Project ER 201124." In.: Stroo Consulting Ashland United States.

61. Taniguchi, Makoto. 2011. *Groundwater and Subsurface Environments: Human Impacts in Asian Coastal Cities* (Springer Science & Business Media).

62. Thornton, Steven F, David N Lerner, and Steven A Banwart. 2001. 'Assessing the natural attenuation of organic contaminants in aquifers using plume-scale electron and carbon balances: model development with analysis of uncertainty and parameter sensitivity', *Journal of contaminant hydrology*, 53: 199-232.

63. Tratnyek, Paul G, Richard L Johnson, Gregory V Lowry, and Richard A Brown. 2014. 'In situ chemical reduction for source remediation.' in, *Chlorinated Solvent Source Zone Remediation* (Springer).

64. Travis, Curtis, and Carolyn Doty. 1990. 'ES&T Views: Can contaminated aquifers at superfund sites be remediated?', *Environmental Science & Technology*, 24: 1464-66.

65. Vodyanitskii, Yu N. 2014. 'Effect of reduced iron on the degradation of chlorinated hydrocarbons in contaminated soil and ground water: A review of publications', *Eurasian soil science*, 47: 119.

66. Vogel, Timothy M, Craig S Criddle, and Perry L McCarty. 1987. 'Transformation of halogenated aliphatic compounds', *Environ. Sci. Technol.;(United States)*, 21.

67. Vörösmarty, Charles J, Pamela Green, Joseph Salisbury, and Richard B Lammers. 2000. 'Global water resources: vulnerability from climate change and population growth', *science*, 289: 284-88.

68. Weber, K. A., L. A. Achenbach, and J. D. Coates. 2006. 'Microorganisms pumping iron: anaerobic microbial iron oxidation and reduction', *Nature Reviews Microbiology*, 4: 752-64.

69. Wiedemeier, Todd H, Barbara H Wilson, Mark L Ferrey, and John T Wilson. 2017. 'Efficacy of an In-Well Sonde to Determine Magnetic Susceptibility of Aquifer Sediment', *Groundwater Monitoring & Remediation*.

70. Wylie, E Miller, Daniel T Olive, and Brian A Powell. 2016. 'Effects of Titanium Doping in Titanomagnetite on Neptunium Sorption and Speciation', *Environmental Science & Technology*, 50: 1853-58.

71. Zektser, S, Hugo A Loáiciga, and JT Wolf. 2005. 'Environmental impacts of groundwater overdraft: selected case studies in the southwestern United States', *Environmental Geology*, 47: 396-404.

72. Zernike, J. 1953. 'The magnetic susceptibilities of pure and slightly oxidized ferrous hydroxide', *Recueil des Travaux Chimiques des Pays-Bas*, 72: 390-94.
73. Zhang, Wei-xian. 2003. 'Nanoscale iron particles for environmental remediation: an overview', *Journal of nanoparticle Research*, 5: 323-32.

74. Zogorski, John S, Janet M Carter, Tamara Ivahnenko, Wayne W Lapham, Michael J Moran, Barbara L Rowe, Paul J Squillace, and Patricia L Toccalino. 2006. 'Volatile organic compounds in the nation's ground water and drinking-water supply wells', *US Geological Survey Circular*, 1292: 101.